Provenance and accommodation pathways of late Quaternary sediments in the deep-water northern Ionian Basin, southern Italy

Article *in* Sedimentary Geology · December 2012

DOI: 10.1016/j.sedgeo.2012.01.007

6 authors, including:

Francesco Perri
Università della Calabria
63 PUBLICATIONS **710** CITATIONS
SEE PROFILE

Salvatore Critelli
Università della Calabria
182 PUBLICATIONS **2,420** CITATIONS
SEE PROFILE

Francesco Muto
Università della Calabria
63 PUBLICATIONS **380** CITATIONS
SEE PROFILE

Silvia Ceramicola
National Institute of Oceanography and Ex…
46 PUBLICATIONS **535** CITATIONS
SEE PROFILE

Sedimentary Geology xxx (2012) xxx–xxx

Contents lists available at SciVerse ScienceDirect

Sedimentary Geology

journal homepage: www.elsevier.com/locate/sedgeo

Provenance and accommodation pathways of late Quaternary sediments in the deep-water northern Ionian Basin, southern Italy

Francesco Perri [a,*], Salvatore Critelli [a], Rocco Dominici [a], Francesco Muto [a], Vincenzo Tripodi [a], Silvia Ceramicola [b]

[a] Università della Calabria, Dipartimento di Scienze della Terra, 87036 Arcavacata di Rende (CS), Italy
[b] Istituto Nazionale di Oceanografia e di Geofisica Sperimentale, Italy

ARTICLE INFO

Article history:
Received 29 August 2011
Received in revised form 11 November 2011
Accepted 13 January 2012
Available online xxxx

Keywords:
Ionian Basin
Northern Calabria
Fluvial systems
Detrital modes
Provenance

ABSTRACT

The northern Calabria along the southeastern coast of Italy provides a favorable setting in which to study complete transects from continental to deep-marine environments. The present northern Ionian Calabrian Basin is a wedge-top basin within the modern foreland-basin system of southern Italy. The Ionian margin of northern Calabria consists of a moderately developed fluvial systems, the Crati and Neto rivers, and diverse smaller coastal drainages draining both the Calabria continental block (i.e., Sila Massif) and the southern Apennines thrust belt (i.e., Pollino Massif). The main-channel sand of the Crati and Neto rivers is quartzofeldspathic with abundant metamorphic and plutonic lithic fragments (granodiorite, granite, gneiss, phyllite and sedimentary lithic fragments). Sedimentary lithic fragments were derived from Jurassic sedimentary successions of the Longobucco Group. The mud samples contain mostly phyllosilicates, quartz, calcite, feldspars and dolomite. Traces of gypsum are present in some samples. The I–S mixed layers, 10 Å-minerals (illite and micas), chlorite and kaolinite are the most abundant phyllosilicates, whereas smectite and chlorite/smectite mixed layers are in small amounts. The geochemical signatures of the muds reflect a provenance characterized by both felsic and mafic rocks with a significant input from carbonate rocks. Furthermore, the degree of source-area weathering was most probably of low intensity rather than moderately intense because CIA values for the studied mud samples are low. Extrapolation of the mean erosion budget from 1 to 25 Ma suggests that at least 5 to 8 km of crust have been removed from the Calabrian orogenic belt and deposited in the marine basins. The Calabrian microplate played an important role in the dynamic evolution of southern Italian fossil and modern basins, representing the key tectonic element of the entire orogenic belt.

1. Introduction

The Calabrian continental margin lies at the SE tip of the arcuate Apennine–Maghrebide accretionary system (e.g. Sartori, 2003). The structural setting of this area is the result of an interplay between the south-eastward migration of the Calabria–Peloritani Arc since the late Miocene and the rapid uplift of onshore and shallow shelf areas since the middle Pleistocene. The Calabria–Peloritani Arc migration resulted in a strong dissection along several NW-trending regional shear-zones, characterized by left lateral movement in the central and northern parts and right-lateral movement in the south (Knott and Turco, 1991).

Two seabed structural settings can be recognized here, the southern Apennine fold-and-thrust belt in the north and the Crotone and Spartivento fore-arc basins in the south. In the northern part of the study area, the Crati River and some minor streams (Trionto, Nicà and Lipuda) feed several wedge-top basins (e.g. Amendolara and Corigliano basins) separated by E–W and NW–SE trending structural ridges (e.g. Amendolara Ridge and Rossano–Cariati High). In the southern area the Neto and Esaro Rivers are the most important drainage basin that feed into the Ionian deep Basin through the Neto and Esaro Canyons separated by Hera Lacinia–Luna High.

The exploration of the seafloor during the last three decades has illustrated the widespread occurrence of submarine depositional systems. The sedimentary fill of basins is related to several factors concerning relationships between source areas and sedimentary basins. Petrography studies of coarse-grained fraction coupled to chemical and mineralogical analyses of the fine-grained fraction represent an important tool for the investigations of the processes occurred from sediment generation on the uplands to the final accommodation on bathyal plain. Detrital modes of sand reflect the cumulative effects of source rock composition, chemical weathering, hydraulic sorting and abrasion (Suttner, 1974; Basu, 1985; Johnsson, 1993; Nesbitt et al., 1996). The correlation of sand composition with weathering intensity (Mann and Cavaroc, 1973; Basu, 1976; Suttner et al., 1981; Velbel, 1985; Cullers et al., 1988) and duration of weathering (Franzinelli and Potter, 1983; Grantham and Velbel, 1988; Stallard, 1988; Johnsson

* Corresponding author.
E-mail address: perri@unibas.it (F. Perri).

0037-0738/$ – see front matter © 2012 Elsevier B.V. All rights reserved.
doi:10.1016/j.sedgeo.2012.01.007

and Stallard, 1989; Johnsson, 1990, 1993; Le Pera and Sorriso Valvo, 2000) has long been established. The distribution of major and trace elements related to the mineralogical composition of fine-grained sediments is a pivotal factor to reconstruct the source-area composition and the weathering and the diagenetic processes (e.g. Condie et al., 1992, 2001; Bauluz et al., 2000; Perri et al., 2005, 2008, 2011a; Mongelli et al., 2006; Critelli et al., 2008; Zaghloul et al., 2010; Caracciolo et al., 2011). By combining the information deduced from the evolution of the X-ray diffraction (XRD) patterns and the elemental analyses for major and trace elements concentrations obtained by X-ray fluorescence spectrometry (XRF) for the mud samples and the petrographic studies for the sand fraction, it is possible to explain and predict the sedimentary evolution and geological processes affecting the studied sediments and, thus, the relationship developed between source area and sedimentary basin.

This study provides insight into the petrology of modern marine sediments, based upon the coupling of both climatic and physiographic controls. Furthermore, the chemical and mineralogical variations provide additional constraints on the behavior of the element distribution during the continental weathering. Knowledge of such coupling is important for the interpretation of analogous clastic deposits in the geological record.

2. Geological setting

The Calabria–Peloritani Arc (CPA) is a fault-bounded terrane connecting the southern Apennines with the Sicilian Maghrebids (Fig. 1). The CPA is composed of pre-Mesozoic crystalline basement and shows evidence of pre-Neogene tectonism and metamorphism. To the northwest, the attenuated continental crust of the CPA grades into the Pliocene–Quaternary oceanic crust of the Tyrrhenian abyssal plain. To the SE, the CPA is delimited by the Ionian subduction zone (Rossi and Sartori, 1981), along which the African plate has been subducted northwestward underneath the CPA (e.g., Cavazza and Ingersoll, 2005 and references therein).

The northwestern portions of the Ionian Sea is characterized by the Taranto Gulf, and it is located offshore along the coast of southern Italy between Calabria and Puglia (Fig. 2). The centrally located Taranto Valley is considered the modern foreland basin of the southern Italy orogenic system, bounded by the autochthonous Adriatic foreland (Apulia Unit), to the east, and the allochthonous fold–thrust Belt of the Southern Apennine Chain and the Calabria–Peloritani Arc terranes, to the west (Rossi and Sartori, 1981; Boccaletti et al., 1984; Critelli, 1999).

The western Taranto Gulf, which belongs to the Calabrian margin, displays a complex morphology that consists of ridges and basins related to the Neogene–Quaternary geodynamic evolution of the submerged, tectonically active extremity of the southern Apennines (Romagnoli and Gabbianelli, 1990). Its structural evolution has been determined mainly by extensional NW–SE and, to a lesser extent, NE–SW trending regional faults (Romagnoli and Gabbianelli, 1990). From west to east, the main morphotectonic features are the Amendolara and Corigliano Basins and the related Amendolara and Rossano–Cariati Ridges, located on the northernmost part of the study area (Fig. 2).

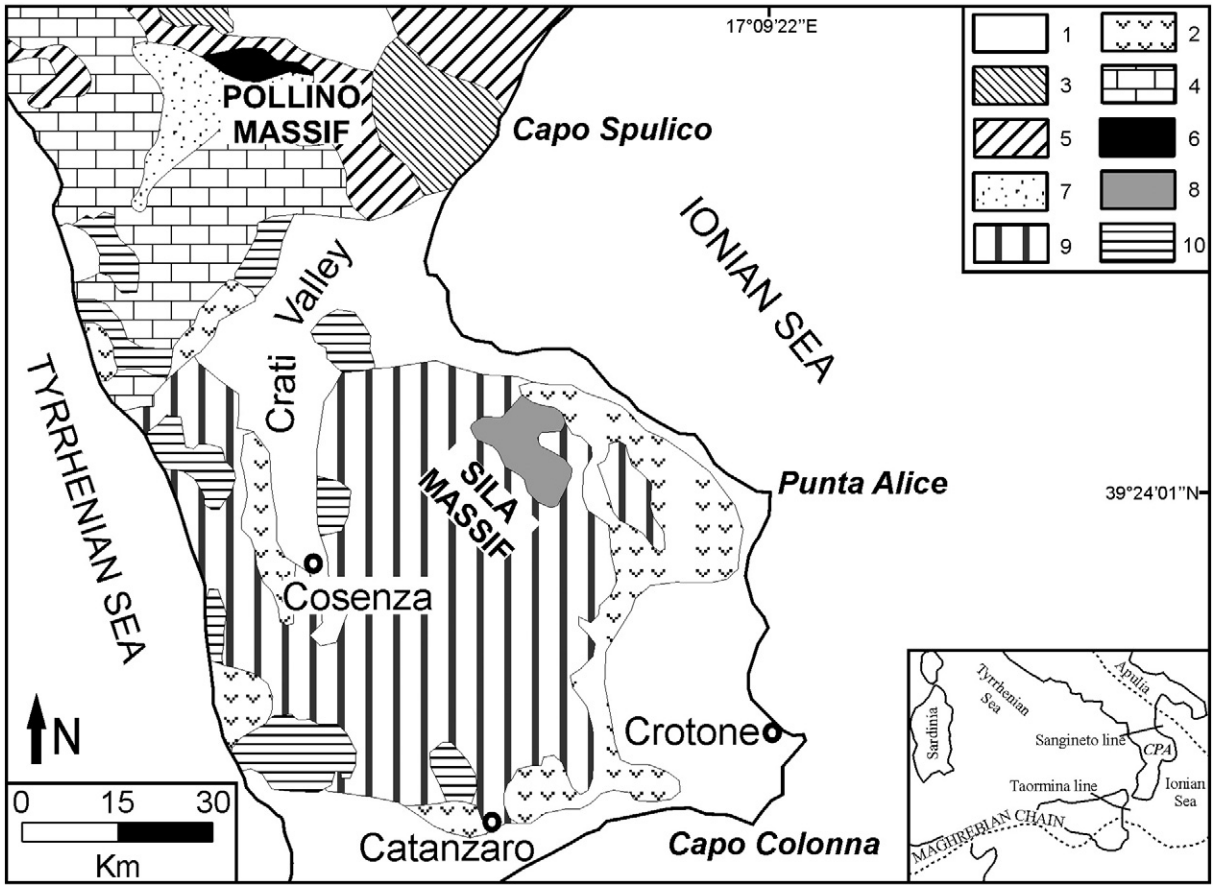

Fig. 1. Geological sketch map of the northern sector of the Calabria–Peloritani Arc (CPA). 1, Pliocene to Holocene sediments, and volcanic and volcaniclastic rocks; 2, Upper Tortonian to Messinian clastics and evaporates; 3, Cilento Group (Middle Miocene); 4, San Donato, Verbicaro and Pollino Units (Triassic to Miocene); 5 to 7, Liguride Complex: 5. Calabro–Lucanian Flysch Unit (Upper Jurassic to Upper Oligocene); 6. Ophiolitiferous blocks and Melange; 7. Frido Unit (Upper Jurassic to Upper Oligocene); 8, Longobucco and Caloveto Groups (Lower Lias to Lower Cretaceous) and Paludi Formation (Upper Oligocene); 9, Sila, Castagna and Bagni basement Units (Paleozoic); 10, Malvito, Diamante–Terranova, Gimigliano Ophiolitiferous units (Upper Jurassic to Lower Cretaceous).
Modified from Critelli (1999) and Perri et al. (2008).

Please cite this article as: Perri, F., et al., Provenance and accommodation pathways of late Quaternary sediments in the deep-water northern Ionian Basin, southern Italy, Sediment. Geol. (2012), doi:10.1016/j.sedgeo.2012.01.007

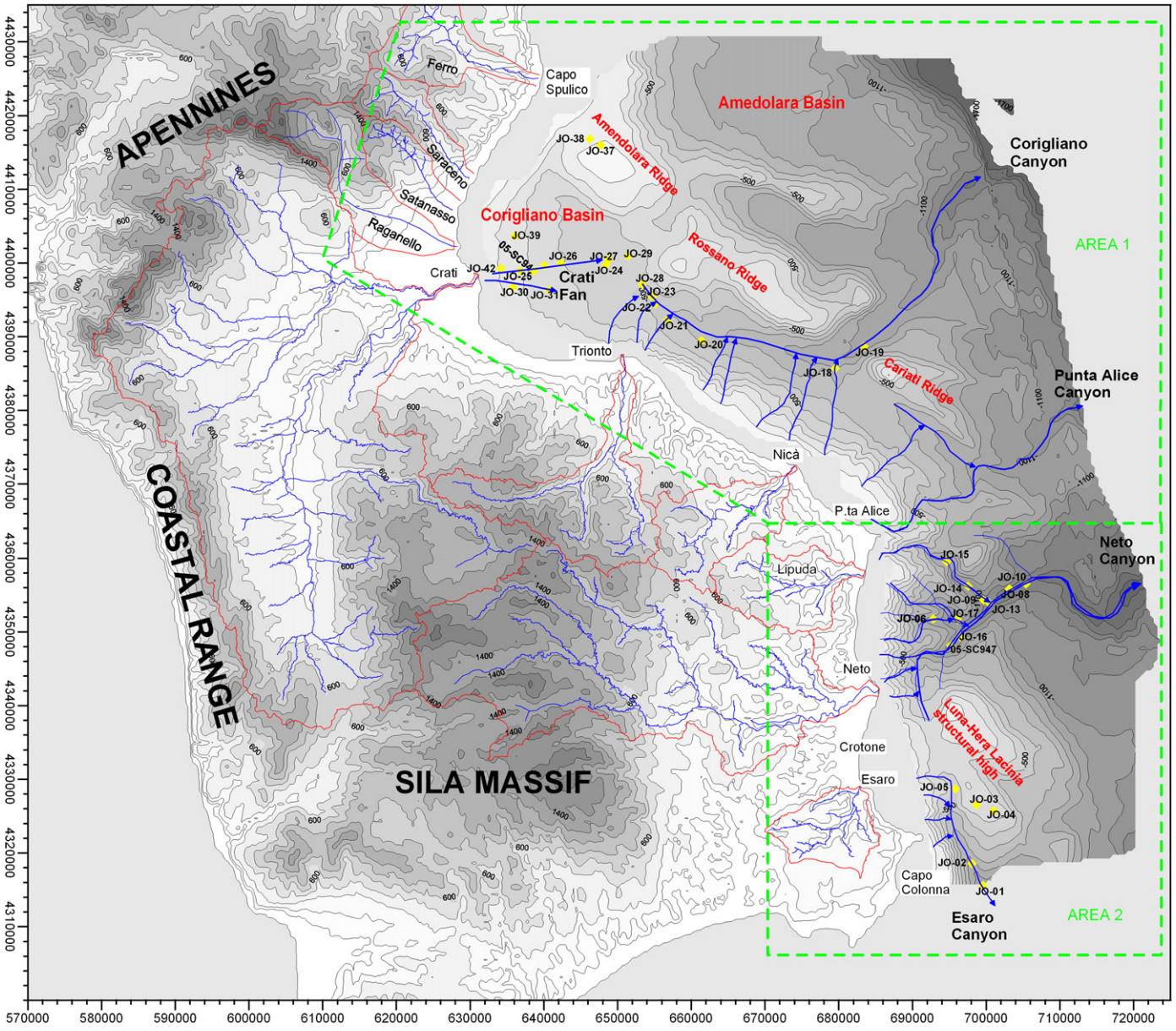

Fig. 2. General sketch map of the investigated area in the Gulf of Taranto. The position of the collected studied samples, mouths of the main rivers along the coasts of the northwestern Gulf of Taranto, and of the Rossano–S. Nicola and Pollino fault systems are also shown.

The northern Ionian Calabrian Basin is characterized by the most important submarine fan, the Crati Fan, and other smaller fans close to the mouth of the Neto River, which developed during the Holocene and connected with the torrential-type deltas on the shelf. The Ionian margin of northern Calabria consists of a moderately developed fluvial system, the Crati and Neto rivers, and diverse smaller coastal drainages draining both the Calabria continental block (i.e., Sila Massif) and the southern Apennines thrust belt (i.e., Pollino Massif) (Fig. 1). The Crati River drains both the Calabrian crustal block and Mesozoic to Tertiary sedimentary terranes of the southern Apennines.

The Sila Massif is a plutonic–metamorphic province, with subordinate sedimentary source rock, producing quartzofeldspathic sand. To the north, additional supplies of sediments are from the Pollino Massif generating sedimentaclastic sand detrital modes reflecting a multicycle provenance from siliciclastic and carbonate strata of the platform-basin tectonostratigraphic units, as well as the Cilento Group and younger sequences (e.g., Critelli, 1999 and references therein).

Additional sources of Quaternary sediment for Ionian basin are submarine structural highs, such as the Amendolara embankment, which borders the Corigliano Basin and produces reworking intrabasinal detritus, and along the promontory of Capo Colonna where a series of Pleistocene terraces have carbonate-rich strata (e.g., Zecchin et al., 2009, 2011 and references therein).

3. Relationship between mainland and coastal-deepwater systems

3.1. Northern sector (Area 2)

The internal sector of the Amendolara bank is a blanketed of 0 to 5 m of carbonate intrabasinal arenites with minor individual glauconite grains or glauconite formed in cavities. The Amendolara bank represents an additional source of quaternary sediments for the Corigliano and Amendolara basins producing reworked intrabasinal detritus. Sediment in the Corigliano Basin is supplied mainly by the Crati River (Romagnoli and Gabbianelli, 1990), and many small coastal drainages such as the Trionto and Saraceno Fiumara rivers.

The Crati River has built a wave-dominated and arcuate fan delta (70 km^2), steep 0.5°–3.0° in relatively shallow-water (200–450 m)

Please cite this article as: Perri, F., et al., Provenance and accommodation pathways of late Quaternary sediments in the deep-water northern Ionian Basin, southern Italy, Sediment. Geol. (2012), doi:10.1016/j.sedgeo.2012.01.007

since 6000–5000 years ago. It occupies the eastern sector of Crati basin which is bounded by NW–SE-trending left-slip faults (Van Dijk et al., 2000; Tansi et al., 2007). The delta is elongated east–west and shows an inner channelized fan and an outer non-channelized fan. The inner fan is characterized by two articulated channelized systems connected to nearshore heads aligned over a front of 3.5 km around the river mouth. The northern channel system is the largest (500–800 m) entrenched and leveed valley, and shows a complex morphology with bottleneck, terraces, thalwegs etc. to 250–300 m below sea-level (b.s.l.), where erosional features are minor related to depositional lobes (non-channelized fan) (Fig. 3g).

The southern channel system is smaller and show erosional features to 200–250 m b.s.l. where sub-bottom profiles show a paleo-valley filled by mud and fine sand probably connected to paleo-mouth of Crati River (Guerricchio and Melidoro, 1975) (Fig. 3h). The outer fan is characterized by depositional lobes separated by interlobe depressions. The northern lobe is characterized by a convex surface to 400 m b.s.l., deflected to the south into Corigliano Canyon and contains some channels up to 2 m deep. The sediment (e.g., JO-28, 29) is composed of mud interbedded with graded sand–silt turbidites (Fig. 3i).

Among the small streams, the Saraceno and Trionto rivers are the most important ephemeral streams (Fiumara) that flow through the mountain chains of Calabria. These streams are very steep, draining mostly mountains, and they are characterized by coastal alluvial fans. The Saraceno Fiumara runs into a mountain valley about 20 km before developing a coastal gravel alluvial fan extending about 3.5 km to the coast and 1.50 km along the coast. The Saraceno Fiumara drains the Pollino Massif, generating sand modes reflecting a multicycle provenance from siliciclastic and carbonate strata of the Panormide, Liguride and Sicilide complexes, as well as the Cilento Group and younger sequences (Fig. 1). The Trionto Fiumara drains the northeastern sector of the Sila Massif, which is composed of low- to medium-grade metamorphic rocks (phyllites — Bocchigliero Unit; micaschist and paragneiss — Mandatoriccio Unit), with a sedimentary cover (conglomerate, arenite, pelite and limestone — Longobucco and Caloveto Groups) and plutonic rocks (granite — Sila Batholite) (Fig. 1). The Trionto Fiumara is cut by several gullies, which by-pass alluvial and littoral sediments (gravel and sand) directly into the Corigliano Canyon and the Taranto Valley (Fig. 3d–f).

Mainland sediment supply for the Corigliano Basin, is mainly derived from the Crati and Trionto River basins. The main-channel sand of the Crati River is quartzofeldspathic (Qm44 F38 Lt18; Qm54 Fk11 Fp35) with abundant metamorphic fragments (Lm96 Lv0 Ls4; Rg18 Rv0 Rm82) (Critelli and Le Pera, 1998). The Pollino Massif is a dominantly siliciclastic and carbonate source area producing sedimentaclastic stream (Qm32 F23 Lt45; Lm5 Lv0 Ls95) and beach (Qm53 F13 Lt34; Lm22 Lv0 Ls78) quartzolithic sand. Detrital modes reflect a multicyclic provenance from siliciclastic and carbonate strata of the southern Apennine tectonostratigraphic units and younger sequences (Critelli, 1999). The Sila Massif is a plutonic–metamorphic province, with subordinate sedimentary source rock, producing quartzofeldspathic stream (Qm33 F34 Lt33; Lm88 Lv0 Ls12) and beach (Qm47 F33 Lt20; Lm94 Lv0 Ls6) sand (Critelli and Le Pera, 1998). Detrital modes reflect strong contributions from granodiorite and granite, gneiss and phyllite; sedimentary lithic fragments are also abundant and derived from Jurassic sedimentary successions (Longobucco Group). Sand of the Trionto River is quartzofeldspathic, with abundant plutonic and metamorphic detritus, and minor sedimentary detritus derived from Jurassic sequences of the Longobucco Group and younger sequences.

3.2. Southern sector (Area 1)

The southern sector, between the Nicà River mouth and Capo Colonna, is approximately 95 km long and consists of two sectors. The shelf and nearshore are supplied by the Nicà River and several small drainages. The source area is chiefly composed of conglomerate, arenite and pelite of the Neogene–Quaternary Cirò Basin, and minor low- to medium-grade metamorphic rocks (phyllites — Bocchigliero Unit; micaschist and paragneiss — Mandatoriccio Unit).

Predominately gneiss and minor plutonic rocks of the Sila Unit constitute the upper Neto drainage system. Lower reaches of the Neto River cut across Miocene to Plio–Pleistocene cover composed mainly of conglomerate, sandstone, calcarenite, marl and clay, and minor evaporites (gypsarenite, carbonate and halite).

The Neto Delta divides the nearshore and shelf-slope depositional systems in two different areas. The northern area is characterized by a narrow shelf cut by gullies, forming a 24 km semicircular Neto–Lipuda canyon head. On the upper slope, three v-shaped tributary canyons, which originate off the mouth of the Neto and Lipuda rivers, converge into two short E–W-trending valleys located between the mouths of the Neto and Lipuda rivers. These three tributary canyons converge into the Neto–Lipuda Canyon at about 1100 m depth. Below the confluence, the canyon is flat-bottomed and runs toward the ENE for about 10 km before forming a marked meander (Fig. 3a–c).

The sand composition of the Neto River is quartzofeldspathic and nearly homogeneous along the main channel, even where the river cuts across a blanket of sedimentary cover. Thus, fluvial transport has not altered sand composition within the Neto drainage basin. Petrographic indices are effective in discriminating between contributions from similar (granite and gneiss) source rocks (Qm/F), in relating the provenance of plutoniclastic and gneissiclastic sand found in the headwaters to grus horizons (Qm/F; Q/Rg), and in distinguishing between upstream first-cycle and downstream multicycle sand (Q/Rg). The uppermost Neto drainage basin is characterized by outcrops of metamorphic and plutonic rocks, whereas sedimentary strata cover the lower reaches of the basin. Thus, there are multiple sources of fluvial sand. Hence, the Neto River detrital modes display a nearly homogeneous quartzofeldspathic composition ($51 \pm 48 \pm 1\%$ QmFLt; $51 \pm 25 \pm 24\%$ QmFkFp in upstream sand; $53 \pm 45 \pm 2\%$ QmFLt; $54 \pm 23 \pm 23\%$ QmFkFp in downstream sand; $46 \pm 45 \pm 9\%$ QmFLt; $51 \pm 16 \pm 33\%$ QmFkFp in coastal sand). However, first-cycle and multicyclic sand can be discriminated using both aphanitic and phaneritic grain types ($90 \pm 10 \pm 0\%$ RgRmRs in first-cycle upstream sand; $61 \pm 25 \pm 14\%$ RgRmRs in multicycled downstream sand; and $66 \pm 27 \pm 7\%$ RgRmRs in coastal sand; Le Pera et al., 2001).

Samples from the Neto delta have similar modal composition to those analyzed from the fluvial system; however, the former are slightly shifted toward the Lt pole on the QmFLt diagram. This shift in composition is produced by an increase in labile metamorphic and carbonate lithic fragments. In addition, delta sands are slightly more enriched in plagioclase (Fp/F 0.62 ± 0.77) than are fluvial sands, whereas the lithic fragment population is similar to that of downstream sand (Le Pera et al., 2001; Bernasconi et al., 2002).

Other clastic contributions to this sector of the Ionian margin of Calabria come from the Nicà and Lipuda rivers. Even if the drainage area of these rivers is modest, they locally contribute clastics to the littoral environment to form fan-delta systems. The Nicà and Lipuda river basins are the only drainage systems generating quartzolithic sand (Qm29 F20 Lt51), where lithic fragments are dominantly low-grade metamorphic and sedimentary.

4. Sampling and methods

Samples analyzed in this study are from two different areas in the northern Ionian Basin (Fig. 2; Table 1). The first area is located between Capo Colonna and Punta Alice; the second area is located between Punta Alice and Capo Spulico (in front of Trionto, Crati and Ferro rivers) (Fig. 2; Table 1). Marine sediments were recovered on board R/V OGS-Explora during the western Gulf of Taranto (WGDT) cruise (21 August–1 September 2005).

Sand samples were washed with dilute H_2O_2 to remove organic matter, air dried and sieved (using 1 F intervals from 4 to

Please cite this article as: Perri, F., et al., Provenance and accommodation pathways of late Quaternary sediments in the deep-water northern Ionian Basin, southern Italy, Sediment. Geol. (2012), doi:10.1016/j.sedgeo.2012.01.007

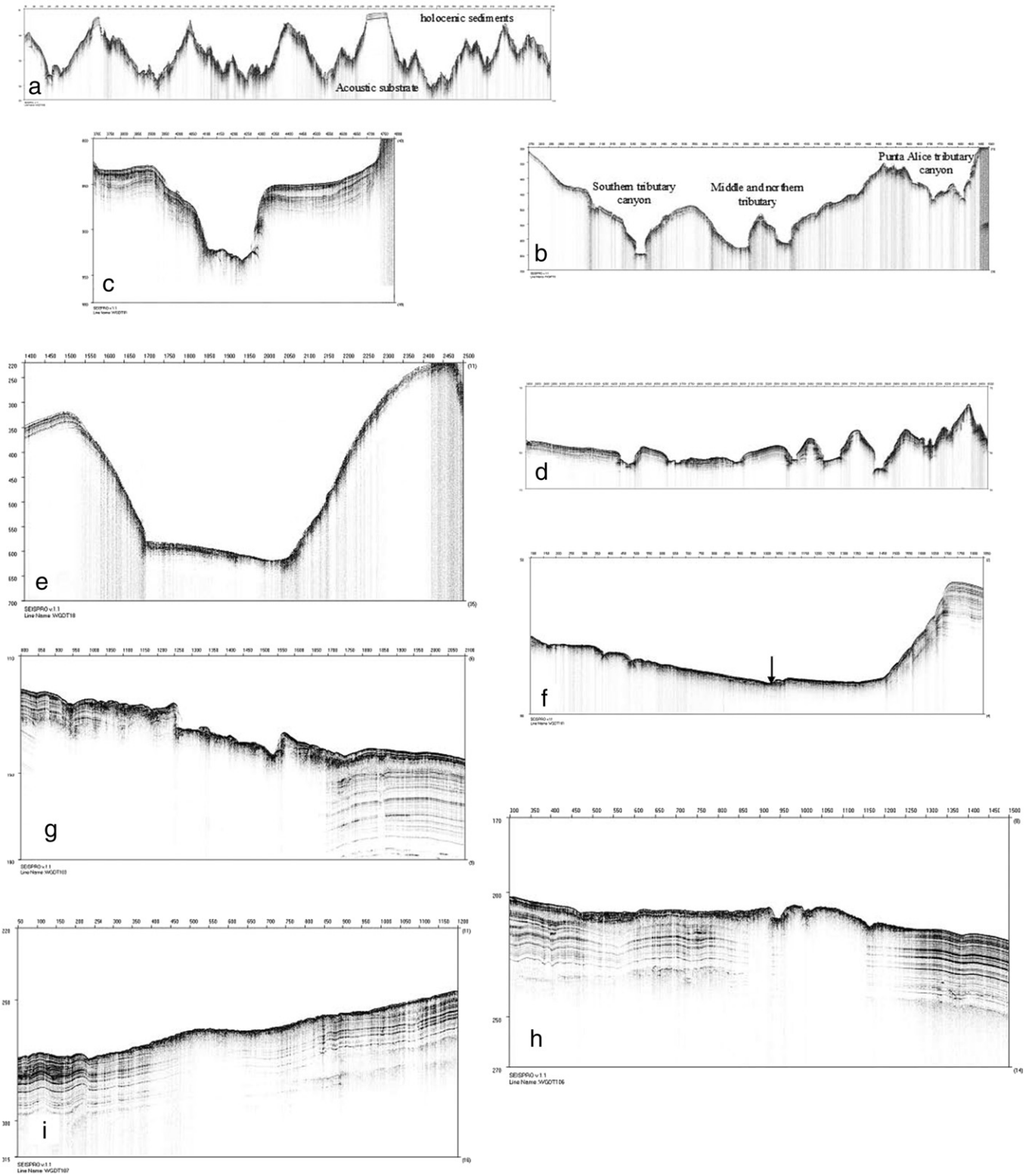

Fig. 3. Sub-bottom profile located along the studied area (see Fig. 1). a) Chirp profile shows an irregular shape characterized by several gullies which cuts olocenic sediment and acoustic substrate, along margin of amphitheater-shaped canyon head. b) Chirp profile is composed, in the middle part of the system, of 4 main tributary which are originating off the mouth of the Neto and Lipuda Rivers and Punta Alice. c) Chirp crossing the U-shaped Neto–Lipuda canyon about 1100 m. d) Shelf margin along Trionto Fan is engraved by several gullies. e) Corigliano canyon cuts trough Rossano and Carioati Ridges. f) The connection between Corigliano Basin and asymmetric profile of the Corigliano Canyon related to Rossano–Cariati Ridges. The arrow point the turbiditic distal system of the Crati Fan. g) In the inner channelized fan the tributaries converge into a major characterized by entrenched and levee valley showing a complex morphology. h) Eastern sector of the Crati submarine fan are characterized by depositional and erosional features. i) The outer sector of Crati fan shows a sand-silty lobes separated by a pelitic interlobe depression.

Please cite this article as: Perri, F., et al., Provenance and accommodation pathways of late Quaternary sediments in the deep-water northern Ionian Basin, southern Italy, Sediment. Geol. (2012), doi:10.1016/j.sedgeo.2012.01.007

Please cite this article as: Perri, F., et al., Provenance and accommodation pathways of late Quaternary sediments in the deep-water northern Ionian Basin, southern Italy, Sediment. Geol. (2012), doi:10.1016/j.sedgeo.2012.01.007

Table. 1
General features and location of pelitic and sand samples of the Ionian Calabria margin, Gulf of Taranto, Southern Italy.

Sample	Latitude	Longitude	X_coord	Y_coord	Depth (m)	Grain-size	Description	Biological contents	Location
JO-01	38° 57′ 59″ N	17° 18′ 13″ E	690,015.269	4,271,971.472	1023	Mud and sand	Graded bed from medium-fine sand to very fine sand and silt; sand is gray in color, and having plant remains and plant root tubes at the base of the sand. The sand bed, few cm in thickness, has turbiditic character and is interbedded into brown mudstone.	plant remains; plant root tubes; algae fragments; planktonic test	Area 1 — Esaro Canyon south of Cape Colonna, canyon located between the coast and the Luna–Hera Lacinia structural high. *Capo-Colonna Province*
JO-02	38° 59′ 36″ N	17° 17′ 11″ E	689,080.195	4,273,914.780	870	Mud	Laminated gray clay with interbedded very thin gray-brown silt and fine sand.	Bivalves	Area 1 — Esaro Canyon south of Cape Colonna, canyon located between the coast and the Luna–Hera Lacinia structural high. Upcurrent with respect JO-01. *Capo-Colonna Province*
JO-03	39° 03′ 54″ N	17° 17′ 46″ E	688,218.004	4,322,955.097	333	Mud	Gray mudstone with interbedded red-brown siltstone–mudstone levels.	Bivalves	Area 1 — Esaro Canyon south of Cape Colonna, canyon located between the coast and the Luna–Hera Lacinia structural high. *Capo-Colonna Province*
JO-04	39° 03′ 27″ N	17° 19′ 20″ E	689,731.402	4,322,691.592	305	mud	Gray mudstone with interbedded red-brown siltstone–mudstone levels.	Bivalves	Area 1 — Esaro Canyon south of Cape Colonna, canyon located between the coast and the Luna–Hera Lacinia structural high. *Capo-Colonna Province*
JO-05	39° 05′ 06″ N	17° 15′ 45″ E	686,438.140	4,324,600.702	538	Mud	Red-brown mudstone with interbedded sandstone–siltstone clasts and dark organic levels.	Bioclasts	Area 1 — Esaro Canyon south of Cape Colonna, canyon located between the coast and the Luna–Hera Lacinia structural high. Upcurrent with respect JO-01–JO-02. *Capo-Colonna Province*
05-SC947	39° 15′ 38″ N	17° 15′ 44″ E	686,157.718	4,336,054.586	1041	Sand	Sample from a core of 3 m in thickness. The core is dominantly pelitic, mostly is hemipelagic mud, mud–siltstone turbidites, and a turbidite sand, medium-size in grain size, slightly laminated.	Planktonic test	Area 1 — Neto Canyon, north of the Neto River mouth. A 3 m in thickness "Core". *Neto–Lipuda Province*
JO-06	39° 17′ 38″ N	17° 14′ 08″ E	684,930.050	4,338,246.559	950	Mud	Gray mudstone with interbedded red-brown siltstone–mudstone levels.	Planktonic test and bivalves	Area 1 — Lipuda Canyon. *Neto–Lipuda Province*
JO-08	39° 19′ 41″ N	17° 21′ 24″ E	691,060.738	4,340,648.192	1344	Sand	Turbidite sand, medium-size, plan-parallel lamination, and gray mud at the top	Planktonic test, and plant remains and organic matter	Area 1 — Neto Canyon, north of the Neto River mouth. Downcurrent with respect JO-09. *Neto–Lipuda Province*
JO-09	39° 18′ 42″ N	17° 19′ 27″ E	689,385.880	4,339,508.025	1280	Mud and sand	Graded bed from medium-fine sand to very fine sand and silt; sand is gray in color, and having plant remains and plant root tubes at the base of the sand. The sand bed, few cm in thickness, has turbiditic character and is interbedded into brown mudstone.	plant remains; plant root tubes; algae fragments; planktonic test	Area 1 — Neto Canyon, north of the Neto River mouth. Downcurrent with respect JO-16 and after confluence of the Punta Alice Canyon. *Neto – Lipuda Province*
JO-10	39° 20′ 02″ N	17° 22′ 58″ E	692,201.436	4,341,353.583	1381	Mud and sand	Graded bed from medium-fine sand to very fine sand and silt; sand is gray in color, and having plant remains and plant root tubes at the base of the sand. The sand bed, few cm in thickness, has turbiditic character and is interbedded into brown mudstone.	plant remains; plant root tubes; algae fragments; planktonic test	Area 1 — Neto Canyon, north of the Neto River mouth. Downcurrent with respect JO-08. *Neto–Lipuda Province*
JO-13	39° 18′ 54″ N	17° 18′ 56″ E	688,769.373	4,339,626.402	1256	Sand	Turbidite sand, medium-size, plan-parallel lamination, and gray mud at the top	Planktonic test	Area 1 — Punta Alice Canyon. Downcurrent with respect JO-14 and close to the confluence with the Neto Canyon. *Neto–Lipuda Province*
JO-14	39° 19′ 58″ N	17° 17′ 32″ E	687,670.606	4,340,754.953	1150	Sand	Turbidite sand, medium-size, plan-parallel lamination, and gray mud at the top	Planktonic test	Area 1 — Punta Alice Canyon. Downcurrent with respect JO-15. *Neto–Lipuda Province*

JO-15	39° 21′ 47″ N	17° 15′ 32″ E	685,893.449	4,342,811.448	941	Mud and sand	Graded bed from medium-fine sand to very fine sand and silt; sand is gray in color, and having plant remains and plant root tubes at the base of the sand. The sand bed, few cm in thickness, has turbiditic character and is interbedded into brown mudstone.	Planktonic test	Area 1 — Punta Alice Canyon. *Neto–Lipuda Province*
JO-16	39° 16′ 15″ N	17° 16′ 38″ E	686,949.643	4,336,928.548	1086	Mud and sand	Graded bed from medium-fine sand to very fine sand and silt; sand is gray in color, and having plant remains and plant root tubes at the base of the sand. The sand bed, few cm in thickness, has turbiditic character and is interbedded into brown mudstone.	Planktonic test	Area 1 — Neto Canyon, north of the Neto River mouth. *Neto–Lipuda Province*
JO-17	39° 17′ 35″ N	17° 16′ 24″ E	686,796.910	4,338,257.547	1063	Mud	Gray mudstone with interbedded red-brown siltstone–mudstone levels.	Planktonic test	Area 1 — Lipuda Canyon. Downcurrent with respect JO-06. *Neto–Lipuda Province*
JO-18	39° 36′ 11″ N	17° 05′ 25″ E	676,830.139	4,358,858.667	850	Mud and sand	Graded bed from medium-fine sand to very fine sand and silt; sand is gray in color, and having plant remains and plant root tubes at the base of the sand. The sand bed, few cm in thickness, has turbiditic character and is interbedded into brown mudstone.	Planktonic test	Area 2 — Nicà Canyon, close to the mouth with the Corigliano Canyon. *Nicà Province*
JO-19	39° 37′ 42″ N	17° 08′ 13″ E	679,278.059	4,360,369.466	929	Mud and sand	Graded bed from medium-fine sand to very fine sand and silt; sand is gray in color, and having plant remains and plant root tubes at the base of the sand. The sand bed, few cm in thickness, has turbiditic character and is interbedded into brown mudstone.	Planktonic test	Area 2 — Corigliano Canyon after confluence of the Nicà Canyon. *Nicà Province*
JO-20	39° 38′ 22″ N	16° 52′ 50″ E	631,342.110	4,360,300.305	628	Mud and sand	Graded bed from medium-fine sand to very fine sand and silt; sand is gray in color, and having plant remains and plant root tubes at the base of the sand. The sand bed, few cm in thickness, has turbiditic character and is interbedded into brown mudstone.	Planktonic test	Area 2 — Trionto Canyon, southern flank. *Trionto Province*
JO-21	39° 39′ 56″ N	16° 49′ 34″ E	628,595.802	4,361,742.018	579	Mud and sand	Graded bed from medium-fine sand to very fine sand and silt; sand is gray in color, and having plant remains and plant root tubes at the base of the sand. The sand bed, few cm in thickness, has turbiditic character and is interbedded into brown mudstone.	Planktonic test	Area 2 — Trionto Canyon, northern flank. *Trionto Province*
JO-22	39° 41′ 09″ N	16° 48′ 29″ E	627,663.709	4,363,425.197	550	Mud and sand	Graded bed from medium-fine sand to very fine sand and silt; sand is gray in color, and having plant remains and plant root tubes at the base of the sand. The sand bed, few cm in thickness, has turbiditic character and is interbedded into brown mudstone.	Planktonic test	Area 2 — Trionto Canyon, northern flank. *Trionto Province*
JO-23	39° 41′ 40″ N	16° 48′ 15″ E	627,537.528	4,363,767.274	560	Mud and sand	Graded bed from medium-fine sand to very fine sand and silt; sand is gray in color, and having plant remains and plant root tubes at the base of the sand. The sand bed, few cm in thickness, has turbiditic character and is interbedded into brown mudstone.	Planktonic test	Area 2 — Trionto Canyon, northern flank. *Trionto Province*
JO-24	39° 44′ 01″ N	16° 43′ 52″ E	623,505.453	4,366,599.580	452	Mud	Gray mudstone with interbedded red-brown siltstone–mudstone levels.	Planktonic test	Area 2 — Crati Fan. Distal portions of the fan (outer fan). *Crati Province*

(continued on next page)

Table. 1 (*continued*)

Sample	Latitude	Longitude	X_coord	Y_coord	Depth (m)	Grain-size	Description	Biological contents	Location
JO-25	39° 43′ 48″ N	16° 35′ 46″ E	616,578.034	4,365,904.059	274	Mud	Gray mudstone with interbedded red-brown siltstone–mudstone levels.	Planktonic test	Area 2 — Crati Fan. In front of the Crati river-mouth. *Crati Province*
JO-26	39° 42′ 36″ N	16° 47′ 22″ E	626,719.499	4,364,819.636	390	Mud and sand	Graded bed from medium-fine sand to very fine sand and silt; sand is gray in color, and having plant remains and plant root tubes at the base of the sand. The sand bed, few cm in thickness, has turbiditic character and is interbedded into brown mudstone.	Planktonic test	Area 2 — Crati Fan. Distal portions of the fan (outer fan). *Crati Province*
JO-27	39° 44′ 28″ N	16° 44′ 07″ E	623,973.984	4,366,906.791	461	Mud	Gray mudstone with interbedded red-brown siltstone–mudstone levels.	Planktonic test	Area 2 — Crati Fan. Distal portions of the fan (outer fan). *Crati Province*
JO-28	39° 42′ 36″ N	16° 47′ 22″ E	626,719.499	4,364,819.636	501	Mud and sand	Graded bed from medium-fine sand to very fine sand and silt; sand is gray in color, and having plant remains and plant root tubes at the base of the sand. The sand bed, few cm in thickness, has turbiditic character and is interbedded into brown mudstone.	Planktonic test	Area 2 — Crati Fan. Distal portions of the fan (outer fan). *Crati Province*
JO-29	39° 44′ 41″ N	16° 46′ 02″ E	625,649.716	4,367,078.068	476	Mud	Gray mudstone with interbedded red-brown siltstone–mudstone levels.	Planktonic test	Area 2 — Crati Fan, middle-fan pelitic facies. *Crati Province*
JO-30	39° 42′ 35″ N	16° 35′ 06″ E	616,252.558	4,364,644.762	271	Mud	Gray mudstone with interbedded red-brown siltstone–mudstone levels.	Planktonic test	Area 2 — Crati Fan. In front of the Crati river-mouth. *Crati Province*
JO-31	39° 42′ 34″ N	16° 38′ 44″ E	619,162.164	4,364,677.770	360	Mud	Gray mudstone with interbedded red-brown siltstone–mudstone levels.	Planktonic test	Area 2 — Crati Fan. In front of the Crati river-mouth. *Crati Province*
JO-37	39° 52′ 52″ N	16° 43′ 39″ E	623,243.249	4,376,042.796	80	Mud	Gray mudstone with interbedded red-brown siltstone–mudstone levels.	Planktonic test	Area 2 — Amendolara Bank. By-pass slope mud deposits
JO-38	39° 53′ 22″ N	16° 42′ 38″ E	622,362.833	4,376,805.930	138	Mud	Gray mudstone with interbedded red-brown siltstone–mudstone levels.	Planktonic test	AREA 2 — Amendolara Bank. By-pass slope mud deposits
JO-39	39° 46′ 20″ N	16° 35′ 15″ E	616,265.983	4,368,918.866	276	Mud	Gray mudstone with interbedded red-brown siltstone–mudstone levels.	Planktonic test	Area 2 — Crati Fan. In front of the Crati river-mouth on the northern flank. *Crati Province*
JO-40	39° 43′ 44″ N	16° 37′ 02″ E	617,921.308	4,365,879.947	316	Mud and sand	Graded bed from medium-fine sand to very fine sand and silt; sand is gray in color, and having plant remains and plant root tubes at the base of the sand. The sand bed, few cm in thickness, has turbiditic character and is interbedded into brown mudstone.	Planktonic test	Area 2 — Crati Fan. In front of the Crati river-mouth. *Crati Province*
JO-41	39° 43′ 49″ N	16° 34′ 32″ E	615,596.740	4,365,900.483	236	Mud and sand	Graded bed from medium-fine sand to very fine sand and silt; sand is gray in color, and having plant remains and plant root tubes at the base of the sand. The sand bed, few cm in thickness, has turbiditic character and is interbedded into brown mudstone.	Planktonic test	Area 2 — Crati Fan. In front of the Crati river-mouth. *Crati Province*
JO-42	39° 43′ 58″ N	16° 35′ 55″ E	616,653.824	4,366,016.209	215	Mud and sand	Graded bed from medium-fine sand to very fine sand and silt; sand is gray in color, and having plant remains and plant root tubes at the base of the sand. The sand bed, few cm in thickness, has turbiditic character and is interbedded into brown mudstone.	Planktonic test	Area 2 — Crati Fan. In front of the Crati river-mouth. *Crati Province*
05-SC948	39° 44′ 06″ N	16° 38′ 46″ E	619,150.073	4,366,586.988	359	Sand	Sample from a core of 3 m in thickness. The core is dominantly pelitic, mostly is hemipelagic mud, mud–siltstone turbidites, and a turbidite sand, medium-size in grain size, slightly laminated.	Planktonic test	Area 2 — Crati Fan. In front of the Crati river-mouth. A 3 m in thickness core. *Crati Province*

0.062 mm). The medium sand fraction (0.50 ± 0.25 mm) was cemented with epoxy and thin-sectioned. Each thin section was etched with HF and stained by immersion in sodium cobalt nitrite solution to allow the identification of feldspars. Alizarine and potassium Fe–cyanide solutions were used for carbonate identification. More than 400 points were counted in each thin section according to the Gazzi–Dickinson method (Gazzi, 1966; Dickinson, 1970; Ingersoll et al., 1984; Zuffa, 1985).

Mud samples were crushed and milled in an agate mill to a very fine powder. The powder was placed in an ultrasonic bath at low power for a few minutes for disaggregation; the <2 μm grain-size fraction was then separated by settling in distilled water.

The mineralogy of the whole-rock powder and clay fractions (<2 μm) was obtained by X-ray diffraction (XRD) using a Bruker D8 Advance diffractometer (CuKα radiation, graphite secondary monochromator, sample spinner; step size 0.02; speed 1 sec for step) at the Università della Calabria (Italy). In order to distinguish chlorite from kaolinite, the samples were heated to 550 °C for 1 h. The heating caused that the intensity of the chlorite {001} reflection to increase greatly, shifting it to about 6.3 to 6.4°2θ. Kaolinite became amorphous to X-rays during this heating, and its diffraction pattern disappeared (Moore and Reynolds, 1997). X-ray diffraction analyses were also carried out on air-dried specimens, glycolated at 60 °C for 8 h, and heated at 375 °C for 1 h (Moore and Reynolds, 1997).

Semiquantitative mineralogical analysis of the bulk rock was carried out on random powders measuring peak areas using the WINFIT computer program (Krumm, 1996). The strongest reflection of each mineral was considered, except for quartz for which the line at 4.26 Å was used instead of the peak at 3.34 Å because of its superimposition with 10 Å-minerals and I–S mixed layer series. The abundance of phyllosilicates was estimated measuring the 4.5 Å peak area. The percentage of phyllosilicates in the bulk rock was split on the diffraction profile of the random powder, according to the following peak areas: 10–15 Å (illite–smectite mixed layers), 10 Å (illite + micas), and 7 Å (kaolinite + chlorite) minerals (Cavalcante et al., 2007).

Elemental analyses for major and some trace elements (Nb, Zr, Y, Sr, Rb, Ba, Ni, Co, Cr, and V) were obtained by X-ray fluorescence spectrometry (Philips PW 1480) at the Università della Calabria (Italy), on pressed powder disks of whole-rock samples (prepared by milling to a fine powder in an agate mill), and compared to international standard-rock analyses of the United States Geological Survey. The estimated precision and accuracy for trace element determinations are better than 5%, except for those elements having a concentration of 10 ppm or less (10–15%). X-ray counts were converted into concentrations by a computer program based on the matrix-correction method according to Franzini et al. (1972, 1975) and Leoni and Saitta (1976a,b). Total loss on ignition (L.O.I.) was determined after heating the samples for 3 h at 900 °C.

5. Results

5.1. Petrography of marine sand

Marine sand includes shallow-marine nearshore and deltaic systems, and deep-marine turbidite systems. Nearshore and deltaic sand is largely influenced by river discharge. The drainage area of the peri-Ionian Calabria margin of the Gulf of Taranto, includes the Crati and Neto rivers and many small coastal drainages, of which the Trionto and Nicà rivers are the major contributors. We attempt here to quantify the composition of the coastal domain of the Ionian Calabrian Basin in order to determine relative effects of the sediment discharge of two large rivers and numerous small coastal drainages (Fig. 2).

Potential sources of sand within the peri-Ionian Basin are the Crati and Neto rivers, and local drainages from the eastern Sila Massif and southern Apennines. The main entry points for sediment into the Ionian Basin include several canyons and gullies. Fluvial sediment input is dominant for the entire borderland, whereas biogenic and aeolian inputs are subordinate. The western Gulf of Taranto is dominated by the Crati submarine fan, the largest fan in this part of the basin.

Sand samples are located in the slope and deep-marine portions of the basin. From south to north, they include sand turbidites in the main canyons of the area. We selected 9 turbidite sand samples from cores and "dredged" samples from the "Neto–Lipuda Canyon system", 12 turbidite sand samples from the Crati Fan (6), and the Trionto (4) and Nicà (2) system.

Sands collected along the southern sector (between Capo Colonna and the Nicà River) range from quartzofeldspathic (Qm36F46Lt18; Neto–Lipuda Province; Fig. 4) to quartzolithic (Qm43F24Lt33; Capo Colonna Province; Fig. 4), with intermediate composition for the Nicà Province (Qm35F33Lt32; Fig. 4). These sands have variable sedimentary versus metasedimentary lithic fragments (Neto–Lipuda: Lm38Lv0Ls62; Capo Colonna Province: Lm33Lv0Ls77; Nicà Province: Lm86Lv0Ls14; Fig. 4). Feldspars (both plagioclase and K-feldspars) are the most abundant constituents (Neto–Lipuda Province: Fp/F of 0.75; Capo Colonna Province: Fp/F of 0.89; Nicà Province: Fp/F of 0.87). Quartz grains are also abundant, mainly as monocrystalline well rounded or subrounded grains, suggesting recycling of sedimentary rocks. Abundant metasedimentary lithic grains include phyllite and fine-grained micaschist. Phaneritic fragments of sandstone grains are also present. Abundant phaneritic fragments of plutonic rocks, mostly plagioclase-rich granodiorite and tonalite, with minor granite, and coarse gneissic fragments also occur; in many samples, they are dominant (Neto–Lipuda: Rg51Rs30Rm19; Capo Colonna Province: Rg32Rs68Rm0; Nicà Province: Rg43Rs9Rm48; Fig. 4). The relative proportions of first-cycle vs. recycled metamorphic and plutonic detritus are difficult to estimate. Accessory minerals are tourmaline, zircon, garnet, hornblende, epidote, sillimanite, andalusite and opaque minerals. Intrabasinal carbonate grains are minor.

Comparing sand modes of the Neto–Lipuda–Nicà deep-marine system with hinterland sand modes of fluvial and coastal environments suggests gradual enrichment of the lithic fragments in the deep-marine environments with respect to hinterland sand. In fact, sand of the Neto River Basin is more feldspar-rich (Le Pera et al., 2001) with respect to deep-marine sand; this may suggest a clastic enrichment from minor drainages draining Tertiary to Quaternary sedimentary successions of the piedmont or coastal areas of the Ionian border. In particular, sedimentary–lithic enrichment occurs (a) at the southern end of the Neto–Lipuda system, where small drainages erode Quaternary and older sedimentary successions, and (b) at the deepest parts of the Neto–Lipuda Canyon system, below confluence of the Lipuda–Punta Alice Canyon within the principal Neto Canyon, generating mixtures of sand of the Neto River (quartzofeldspathic) with sand of the Lipuda and local rivers (quartzolithofeldspathic sand with more sedimentary detritus).

Sands collected along the northern sector (between the Trionto River and Capo Spulico) have similar compositions: sands from Crati Province are metamorphiclastic (Rg14Rs19Rm67) and quartzofeldspathic (Qm34F41Lt25) with abundant metamorphic and plutonic grains; sands from Trionto Province are metamorphiclastic (Rg11Rs16Rm73) and quartzofeldspathic (Qm38F27Lt35) with abundant metamorphic grains. These sands are rich in aphanitic metasedimentary lithic fragments (Trionto Province: Lm90Lv0Ls10; Crati Province: Lm75Lv0Ls25; Fig. 4). Feldspars are the most abundant constituents (Trionto Province: Fp/F 0.97; Crati Province: Fp/F 1.16). Quartz grains are also abundant, mainly as monocrystalline well rounded or subrounded grains, suggesting recycling of sedimentary rocks. Abundant metasedimentary lithic fragments include phyllite and fine-grained micaschist. Sedimentary lithic grains, including shale, mudstone, siltstone and carbonate rocks, are abundant in samples of the drainage basins derived from the southeastern flank of the southern Apennines. Other sedimentary lithic fragments are

Please cite this article as: Perri, F., et al., Provenance and accommodation pathways of late Quaternary sediments in the deep-water northern Ionian Basin, southern Italy, Sediment. Geol. (2012), doi:10.1016/j.sedgeo.2012.01.007

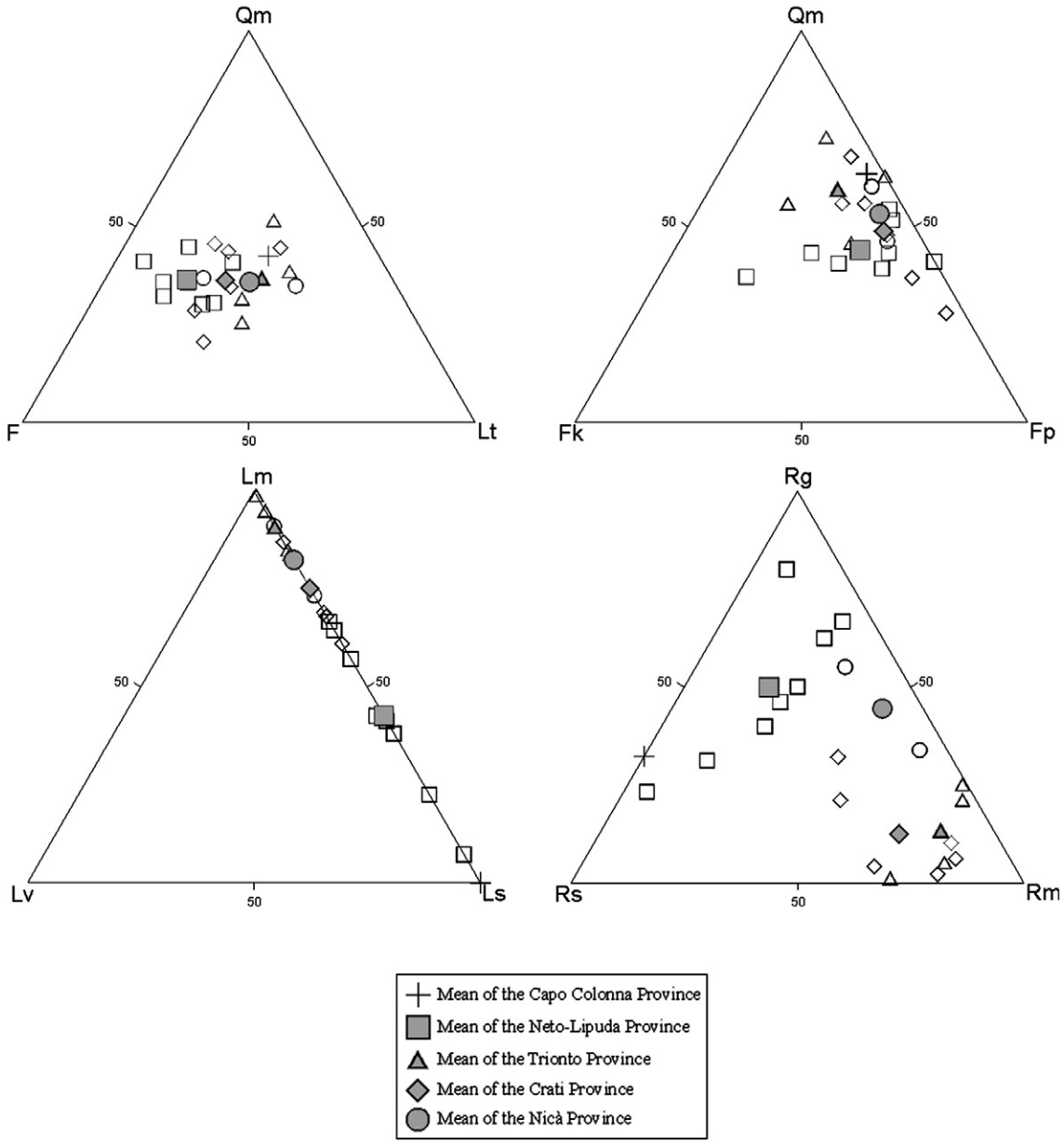

Fig. 4. Ternary plots for the sand studied samples of Qm (monocrystalline quartz), F (feldspars) and Lt (aphanitic lithic fragments); Qm (monocrystalline quartz), Fk (K-feldspar) and Fp (plagioclase); Lm (metamorphic), Lv (volcanic) and Ls (sedimentary) lithic fragments; Rg (plutonic rock fragments), Rs (sedimentary rock/lithic fragments) and Rm (metamorphic rock fragments). See the text for more details. Each open symbol represents the individual sand sample of the studied province.

delivered by the Trionto and Nicà Rivers, and other minor drainages eroding the Jurassic Longobucco Group and Cenozoic to Quaternary strata of the Rossano Basin and the Cariati Thrust Unit (e.g., Critelli, 1999; Barone et al., 2008; Critelli et al., 2011).

The sand modes of the Crati–Trionto deep-marine system are quite similar in composition with the hinterland sand modes at fluvial and coastal environment. Sands of the main channel of the Crati River, the deltaic system and the Crati Fan are similar, with only a few percent of enrichment in quartz with increasing maturity and amalgamation by transport (Critelli and Le Pera, 2003 and present data). Also, sand modes of the Trionto and Nicà rivers are similar to those of turbidite sand of the Trionto and Nicà canyons (Critelli and Le Pera, 2003). This suggest that the Crati, Trionto and Nicà rivers represent the key single source for sediment delivered into the canyons and the Corigliano Basin, with no evidence of mixing and amalgamation within the basin.

5.2. Mineralogy of marine mud

Whole-rock XRD analyses (Table 2) indicate that phyllosilicates are the main mineralogical components, ranging from 32% to 57% of the bulk rock. The non-phyllosilicate minerals are represented by quartz, carbonate minerals (calcite and dolomite) and feldspars (plagioclase and K-feldspar). A few samples contain gypsum. Quartz ranges from 27% to 39%. K-feldspar has low concentration, with values up to 5%, whereas plagioclase ranges from a few percent up to 12%. Dolomite is present in all samples, with an average value of 2%, whereas calcite ranges from 7% to 19%. Variation of mineral concentrations is related to the different source areas that influence the chemical and mineralogical composition of the sediments. The <2 μm grain-size fraction is mainly composed of I–S mixed layers. Illite is present in variable amounts. Chlorite and kaolinite contents usually are low. Only small amounts of C–S mixed layers occur.

Please cite this article as: Perri, F., et al., Provenance and accommodation pathways of late Quaternary sediments in the deep-water northern Ionian Basin, southern Italy, Sediment. Geol. (2012), doi:10.1016/j.sedgeo.2012.01.007

Table. 2
Results of whole rock XRD analyses for the studied mud samples.

Samples	∑phy	Plg	K-feld	Dol	Calc	Qtz	Gyp
JO01	45	4	3	2	17	28	1
JO02	46	4	2	2	17	29	0
JO03	48	4	2	3	13	28	1
JO04	48	4	2	3	14	28	0
JO05	48	4	2	2	14	28	1
JO06	43	5	2	2	14	32	1
JO09	32	11	5	2	13	37	0
JO10	36	10	3	2	14	33	2
JO15	32	9	4	2	13	39	1
JO16	37	10	4	2	12	34	1
JO17	45	5	2	3	13	31	0
JO18	55	4	2	3	8	27	tr
JO19	54	4	2	3	8	29	0
JO20	54	4	1	3	8	30	0
JO21	50	6	4	2	7	31	0
JO22	53	5	1	2	8	30	1
JO23	53	4	1	3	8	31	0
JO24	57	4	1	2	8	28	0
JO25	54	5	1	2	8	29	tr
JO26	52	5	1	3	10	29	0
JO27	57	4	1	2	8	27	1
JO28	54	3	1	3	8	30	1
JO29	55	3	2	3	8	29	0
JO30	53	5	1	3	10	28	1
JO31	55	4	1	3	8	29	0
JO37	45	3	1	2	19	29	0
JO38	49	4	1	2	15	28	0
JO39	53	5	1	2	8	30	tr
JO40	50	12	1	2	8	27	0
JO41	53	4	1	2	10	30	0
JO42	52	4	2	3	8	30	tr
Minimum	32	3	1	2	7	27	0
Maximum	57	12	5	3	19	39	2
Average	49	5	2	2	11	30	0
SD	7	2	1	0	3	3	1

5.3. Whole-rock geochemistry of marine mud

Major- and trace-element concentrations are listed in Table 3 and in Table 4. The studied muds have been plotted (Fig. 5) in the classification diagram for clastic rocks (Herron, 1988). The SiO_2/Al_2O_3 ratio, the most commonly used parameter, reflects the relative abundance of quartz, feldspar and clay minerals (e.g., Potter, 1978). The studied samples plot in the field of shale, toward the wacke field, thus reflecting variation in the quartz–feldspars/mica ratio in individual samples; only one sample (JO09) falls in the wacke field (Fig. 5).

Geochemical compositions of the studied mud samples were normalized to the Global Subducting Sediment (GLOSS; Plank and Langmuir, 1998). GLOSS is dominated by terrigenous material (76 wt.% terrigenous, 7 wt.% calcium carbonate, 10 wt.% opal, 7 wt.% mineral-bound H_2O^+), and therefore similar to the upper continental crust (UCC; McLennan et al., 2006) in composition (Plank and Langmuir, 1998). The general trend of the observed patterns (Fig. 6) shows similar variations for the studied muds. The chemical differences between the studied samples can be described as follows: samples of the southern sector (area located between Capo Colonna and Punta Alice) generally show lower values of Fe, Ni, Ti, V and Cr and higher values of Ca, Sr and, partially, Si (Fig. 6a); samples of the northern sector (area located between Punta Alice and Capo Spulico) generally show higher values of Fe, Ni, Ti, V and Cr and lower values of Ca and Sr (Fig. 6b). Two samples (JO37 and JO38) of the pattern b (Fig. 6b) have a trend comparable to the pattern a samples (Fig. 6a).

In a ternary plot of SiO_2 (representing quartz or opaline silica), Al_2O_3 (representing mica/clay minerals), and CaO (representing carbonate), the sediments of the southern sector can be described as mixtures of biogenous carbonate with an aluminosilicate component (Group 1; Fig. 7), but sediments of the northern sector show homogeneous composition characterized by slightly higher Al content (e.g., Group 2; Fig. 7) than average shale (in particular GLOSS and UCC). Samples JO37 and JO38 (northern sector) are two outliers since they show a general trend similar to the southern sector samples. These chemical associations and elemental variations are related to the mineralogical composition of the studied muds, as shown above by the mineralogical analyses.

6. Discussion

The composition and variation of the studied marine sediments, based on mud geochemistry and mineralogy coupled with sand petrography, suggest that these sediments are mainly related to two different source areas. The first source is mainly characterized by carbonate, since most of the marine mud samples contain the highest concentration of Ca, that is almost 2 times higher than the UCC (McLennan et al., 2006). To the north (Area 2: between Punta Alice and Capo Spulico; Table 1; Fig. 2), samples JO37–JO38 are derived by both intrabasinal reworking of the topographic highs (Amendolara Ridge) along a small 'patch reef', and by recycling of old (Mesozoic to Tertiary) extrabasinal carbonates of the Pollino Massif. Sand detrital modes reflect a multicyclic provenance from siliciclastic and carbonate strata of the southern Apennines fold–thrust belt. To the south (Area 1a: between Capo Colonna and Punta Alice, below to Neto–Lipuda Canyon; Table 1; Fig. 2), samples JO01–JO05, and samples JO06 and JO17 (Area 1b: between Capo Colonna and Punta Alice, close to and above to Neto–Lipuda Canyon; Table 1; Fig. 2) contain high values of CaO that can be related to recycling of Pleistocene marine terraces of the Crotone Peninsula.

The first sector (Area 1b: between Capo Colonna and Punta Alice, close to and above to Neto–Lipuda Canyon; Table 1; Fig. 2) is characterized by samples influenced the Sila Massif plutonic–metamorphic province, with subordinate sedimentary source rocks, producing quartzofeldspathic stream and beach sand. Detrital modes indicate strong contributions from granodiorite and granite, gneiss, and phyllite; abundant sedimentary lithic fragments were derived from Jurassic sedimentary successions (the Longobucco Group; Perri et al., 2008).

The second sector (Area 2: between Punta Alice and Capo Spulico, in front of Trionto, Crati and Ferro rivers; Table 1; Fig. 2) contain marine muds showing the highest concentration of Al that is almost 1.2 times higher than the UCC (McLennan et al., 2006). Aluminum is generally considered an indicator of high detrital input. Very low concentrations of Al, and also of Fe, in sediment in comparison with those of the UCC (McLennan et al., 2006) is indicative of low detrital input. An increase in the concentration of Al might be attributed to higher erosion rates (e.g., Karbassi and Amirnezhad, 2004). The Al values of marine muds of the second sector might be attributed to higher erosion rates, related to the Crati River fluvial system (Fig. 2). The relationship among Al and the other major and trace elements is related to the cation exchange and sorption reactions that clay minerals undergo in seawater (e.g., Elderfield, 1976). Mineralogical analyses also show abundant phyllosilicate contents for these sediments. Furthermore, marine muds of the second sector show the highest Ti, Ni, Cr and Nb (Fig. 6) contents, suggesting a mafic supply for these sediments. This sector (Area 2: between Punta Alice and Capo Spulico, in front of Trionto, Crati and Ferro rivers; Table 1; Fig. 2) is influenced by the Crati River and the diverse smaller coastal drainages of the Calabria continental block (i.e., Sila Massif, mostly drained by the Trionto River) and the southern Apennines thrust belt (i.e., Pollino Massif mostly drained by Ferro River), that mainly supply siliciclastic materials with a moderate mafic contribution.

The mud samples also contain significant amounts of La and Ce. It is well know that the bulk of the REEs (Rare Earth Elements) found in the clastic sediments are found in the finer grained fractions, where their distributions are most similar to the REE distributions found in the source rocks (Cullers et al., 1987). Together, the contents and

Please cite this article as: Perri, F., et al., Provenance and accommodation pathways of late Quaternary sediments in the deep-water northern Ionian Basin, southern Italy, Sediment. Geol. (2012), doi:10.1016/j.sedgeo.2012.01.007

Table 3
Major and trace element concentrations for the studied mud samples.

Sample	JO01	JO02	JO03	JO04	JO05	JO06	JO09	JO10	JO15	JO16	JO17	JO18	JO19	JO20	JO21
Oxides (wt.%)															
SiO_2	45.55	47.21	45.44	44.75	46.01	47.87	57.79	50.39	50.64	51.07	48.03	46.74	45.59	46.77	49.52
TiO_2	0.63	0.66	0.73	0.72	0.72	0.72	0.51	0.61	0.60	0.64	0.70	0.80	0.81	0.78	0.74
Al_2O_3	13.13	13.65	14.94	14.43	14.22	14.37	12.15	12.61	12.75	13.82	14.20	16.42	16.41	15.79	15.54
Fe_2O_3	4.24	4.49	5.56	5.37	5.35	5.18	3.23	3.71	3.76	4.49	5.07	6.26	6.18	5.92	5.37
MnO	0.28	0.10	0.15	0.19	0.12	0.09	0.12	0.10	0.09	0.10	0.10	0.12	0.14	0.11	0.14
MgO	3.46	3.41	3.49	3.46	3.44	3.35	2.80	3.44	3.42	3.16	3.33	3.49	3.51	3.46	3.71
CaO	10.23	10.54	8.46	9.00	8.59	8.56	9.08	9.29	8.52	8.27	8.75	6.24	6.12	6.21	5.81
Na_2O	2.82	1.98	1.86	2.35	2.35	2.17	2.42	3.98	4.24	2.31	1.98	2.01	2.26	2.45	3.18
K_2O	2.50	2.59	2.82	2.75	2.70	2.82	2.69	2.68	2.73	2.79	2.74	3.13	3.13	3.04	2.98
P_2O_5	0.13	0.14	0.14	0.14	0.14	0.14	0.14	0.15	0.14	0.14	0.15	0.13	0.14	0.14	0.14
LOI	17.00	15.19	16.38	16.83	16.33	14.70	9.03	13.04	13.03	13.19	14.92	14.64	13.69	15.31	12.88
Total	99.96	99.97	99.97	99.99	99.98	99.98	99.94	99.98	99.91	99.98	99.98	99.98	97.98	99.98	100.01
Trace elements (ppm)															
V	137	138	168	165	159	148	70	100	100	120	143	172	163	163	137
Cr	89	96	117	112	111	104	43	67	65	66	101	128	117	119	92
Co	14	14	19	18	17	15	5	9	10	11	14	20	19	17	16
Ni	53	58	68	70	70	61	28	40	36	40	55	69	68	67	59
Cu	21	18	20	22	24	21	13	13	14	17	22	27	29	21	23
Zn	115	107	135	124	156	122	67	89	83	112	122	143	138	139	123
Rb	115	119	131	128	130	130	102	115	116	125	128	148	145	141	132
Sr	415	384	323	350	314	314	263	324	295	308	320	240	235	233	229
Ba	299	298	336	311	313	359	378	376	381	387	352	398	437	424	417
Y	29	30	29	32	31	34	32	28	26	29	31	32	33	30	32
Zr	149	158	130	134	132	159	148	181	153	167	166	145	172	144	158
Nb	14	14	15	15	15	15	11	13	13	14	15	16	16	16	15
La	25	26	31	34	29	20	8	15	22	23	31	38	39	39	25
Ce	70	71	80	84	74	76	44	57	56	65	77	91	96	89	76
Chemical Index of Alteration (Nesbitt and Young, 1982)															
CIA	62.14	65.17	66.9	64.52	64.61	65.35	56.91	53.64	53.54	60.94	64.45	64.46	64.46	62.95	58.92

distributions of the transition elements (e.g., Cr and Ni) and the LREEs (Light Rare Earth Elements; e.g., La and Ce) may provide useful indices of chemical differentiation that may allow the recognition of different provenance areas. These indices, including LREEs/M ratios, where M is a transition element, reflect the greater input of felsic rocks with a modest mafic contribution mostly for the mud samples of the Area 2 (Table 5). The mafic supply is mainly related to both metamorphic and ophiolitic rocks drained by the Crati River (e.g., Critelli and Le Pera, 2003).

Biogenic carbonate production is inhibited by the presence of clastic material, so in areas of low input of detritus from rivers or by ocean currents, there is the potential for carbonate deposition (Nichols, 1999). The marine muds of this sector (Area 2: between Punta Alice and Capo Spulico, in front of the Trionto, Crati and Ferro rivers; Table 1; Fig. 2) are characterized by minor carbonate (Table 2) probably due to abundant clastic detritus.

Chemical weathering strongly affects major-element geochemistry and mineralogy of clastic sediments (e.g., Nesbitt and Young, 1982; Johnsson et al., 1988; McLennan and Taylor, 1991). Quantitative measures, such as the chemical index of alteration (CIA; Nesbitt and Young, 1982), are useful to evaluate the degree of chemical weathering. Calculation of this index incorporates only the CaO present in silicate minerals. The marine mud samples show very low values of CIA (average = 62.68 ± 3.42) suggesting low weathering for the source areas. Intense chemical weathering results in the removal of labile cations (e.g., Ca^{2+}, Na^{+}, K^{+}) relative to stable residual constituents (Al^{3+}, Ti^{4+}) during weathering (Nesbitt and Young, 1982), due to the conversion of feldspars to clay minerals. The marine muds contain abundant mobile elements, such as Ca, Na, Mg and K that are commonly higher than the GLOSS (Plank and Langmuir, 1998) composition (Fig. 6). Furthermore, these sediments are characterized by abundant feldspars (at least 13–16%; Table 2) in many samples. Thus, the chemistry and mineralogy of the studied marine muds suggest that these sediments have been produced from source areas characterized by a low intensity of weathering related to a temperate climate such that occurring in the Mediterranean.

Table 4
The oxide values reported on LOI-free basis.

Sample	JO01	JO02	JO03	JO04	JO05	JO06	JO09	JO10	JO15	JO16	JO17	JO18	JO19	JO20	JO21
Oxides LOI-free (wt.%)															
SiO_2	50.05	51.57	50.95	49.44	51.22	52.15	61.61	52.94	53.62	54.80	53.18	51.68	52.16	52.18	51.15
TiO_2	0.69	0.72	0.82	0.80	0.80	0.79	0.54	0.64	0.63	0.69	0.78	0.89	0.89	0.87	0.76
Al_2O_3	14.43	14.90	16.75	15.94	15.83	15.65	12.95	13.25	13.50	14.83	15.72	18.16	17.99	17.62	16.05
Fe_2O_3	4.66	4.90	6.23	5.93	5.96	5.65	3.45	3.90	3.98	4.82	5.61	6.92	6.77	6.61	5.54
MnO	0.31	0.11	0.17	0.21	0.13	0.10	0.13	0.10	0.09	0.11	0.11	0.14	0.15	0.13	0.15
MgO	3.80	3.72	3.91	3.82	3.83	3.65	2.99	3.62	3.62	3.39	3.68	3.86	3.85	3.87	3.83
CaO	11.24	11.52	9.49	9.94	9.57	9.33	9.68	9.76	9.02	8.87	9.69	6.90	6.70	6.93	6.00
Na_2O	3.10	2.17	2.09	2.60	2.62	2.37	2.58	4.18	4.49	2.48	2.20	2.22	2.48	2.73	3.28
K_2O	2.75	2.83	3.16	3.04	3.01	3.08	2.87	2.82	2.90	3.00	3.04	3.46	3.43	3.39	3.08
P_2O_5	0.14	0.15	0.16	0.15	0.16	0.16	0.15	0.15	0.14	0.16	0.16	0.15	0.15	0.15	0.14
LOI	17.00	15.19	16.38	16.83	16.33	14.70	9.03	13.04	13.03	13.19	14.92	14.64	13.69	15.31	12.88

Please cite this article as: Perri, F., et al., Provenance and accommodation pathways of late Quaternary sediments in the deep-water northern Ionian Basin, southern Italy, Sediment. Geol. (2012), doi:10.1016/j.sedgeo.2012.01.007

JO22	JO23	JO24	JO25	JO26	JO27	JO28	JO29	JO30	JO31	JO37	JO38	JO39	JO40	JO41	JO42
50.28	48.83	46.84	46.00	46.60	46.76	47.37	46.41	47.11	46.72	41.98	47.19	47.25	45.81	48.27	47.06
0.80	0.78	0.81	0.76	0.79	0.80	0.81	0.79	0.78	0.80	0.71	0.78	0.81	0.76	0.78	0.78
16.11	15.98	16.48	15.39	15.73	16.31	16.32	15.88	15.53	16.10	13.49	14.61	16.36	15.20	15.71	15.29
5.94	5.70	6.26	5.79	6.03	6.28	5.99	6.01	5.94	6.27	4.68	5.92	6.11	5.71	5.85	6.03
0.12	0.14	0.13	0.11	0.10	0.13	0.12	0.13	0.10	0.12	0.08	0.10	0.09	0.10	0.09	0.10
3.36	3.57	3.60	3.59	3.62	3.60	3.71	3.73	3.55	3.65	3.36	3.53	3.57	3.73	3.51	3.58
5.66	6.60	6.14	7.27	7.19	6.39	6.16	6.39	7.39	6.54	11.03	8.89	6.65	6.69	7.04	7.15
2.13	2.55	2.17	2.47	2.02	1.85	2.73	2.58	2.13	2.12	2.12	1.99	1.95	3.01	1.96	2.56
3.12	3.05	3.05	2.83	2.80	2.92	3.11	2.89	2.74	2.90	2.40	2.70	2.97	2.75	2.78	2.67
0.14	0.14	0.13	0.14	0.14	0.13	0.14	0.13	0.14	0.14	0.13	0.13	0.13	0.13	0.14	0.14
12.33	12.65	14.39	15.63	14.98	14.79	13.53	15.06	14.59	14.62	19.98	14.66	14.07	16.09	13.82	14.60
99.99	99.99	100.00	99.98	100.00	99.96	99.99	100.00	100.00	99.98	99.96	100.50	99.96	99.98	99.95	99.96
147	154	176	166	172	174	163	166	168	171	163	169	171	163	163	162
105	110	129	113	126	141	121	131	124	127	109	110	130	123	120	125
18	17	20	19	17	21	18	20	19	21	13	16	21	19	19	19
66	63	75	67	68	74	67	72	68	66	62	65	73	64	64	66
27	29	28	22	27	31	25	18	27	27	25	28	34	22	23	25
133	130	134	129	135	133	134	128	133	138	121	127	133	124	130	128
144	141	146	135	135	141	143	136	131	139	118	132	144	128	132	125
220	240	230	265	264	235	236	233	260	241	593	415	243	263	256	257
450	394	379	355	348	358	397	356	371	372	269	319	354	351	376	350
34	30	32	29	32	31	31	30	31	31	33	30	31	28	31	30
168	149	144	128	147	142	162	137	145	143	158	140	145	137	145	143
16	15	16	16	16	16	16	15	16	16	15	16	16	15	16	15
29	32	39	37	32	39	41	40	30	36	18	36	29	22	36	35
81	71	98	86	90	96	88	88	82	88	81	92	92	81	84	83
65.38	61.58	64.5	59.18	65.93	64.67	62.66	62.62	64.51	64	65.24	65.75	63.32	59.03	65.66	60.16

7. General implications and conclusions

The Ionian margin of Calabria is an exceptional area in which sedimentation and sediment composition can be examined in the total environmental context. The Ionian side of Calabria provides diverse modern systems extending from high-elevation source areas to deep-marine basins, all of which can be used as modern analogs to ancient systems. Thus, direct comparison can be made between modern sand and ancient sandstone, and paleogeographic and paleotectonic reconstructions can be constrained.

Alluvio–fluvial and deltaic systems of the Ionian side of northern Calabria generate dominantly quartzofeldspathic sand, reflecting the dominantly plutoniclastic and metamorphiclastic nature of the key source massif of the area, the Sila Mountains. Other local sources are the south-eastern flank of the Southern Apennines and Neogene sequences of the Peri-Ionian piedmont. Sediment composition and mud geochemistry and mineralogy identifies four main source areas for late Quaternary turbidites of the Ionian margin. The turbidites originate from fluvial sources of northern Calabria and are introduced through moderate to small canyons. Deep-marine sands of the Ionian margin are quartzofeldspathic, which reflects the dominant mainland sources of the Crati (northern) and Neto (southern) rivers, with lesser contributions from small drainage systems such as the Trionto and Nicà rivers.

In detail, the northern studied area, the Gulf of Sibari, is sedimentologically and compositionally dominated by the Crati Fan, a sand–mud turbidite system represented by quartzofeldspathic sand quite similar in composition to the mainland source of the Crati River main-channel and its river-mouth. Local contributions to the deep-marine environment are derived from the (a) Trionto River, generating quartzofeldspathic sand turbidites, and the (b) intrabasinal source from the Amendolara bank, generating intrabasinal carbonate sand. In the southern studied area, canyons and gullies dominate morphologically, and the main source for turbidites was the Neto River. Sand–mud turbidites are compositionally quite similar to the quartzofeldspathic Neto River and delta; local contributions are from quartzolithic

JO22	JO23	JO24	JO25	JO26	JO27	JO28	JO29	JO30	JO31	JO37	JO38	JO39	JO40	JO41	JO42
53.42	52.11	51.53	51.31	51.84	52.22	51.34	51.41	52.12	51.74	48.21	52.57	52.48	50.96	52.85	51.66
0.85	0.83	0.89	0.85	0.88	0.90	0.87	0.87	0.87	0.88	0.82	0.87	0.90	0.84	0.85	0.86
17.11	17.06	18.13	17.17	17.50	18.22	17.69	17.60	17.18	17.83	15.50	17.39	18.19	16.91	17.20	16.79
6.31	6.08	6.89	6.46	6.71	7.01	6.50	6.66	6.57	6.94	5.37	6.59	6.79	6.36	6.41	6.62
0.13	0.15	0.14	0.12	0.11	0.14	0.13	0.14	0.11	0.13	0.09	0.11	0.10	0.12	0.10	0.11
3.57	3.81	3.96	4.00	4.03	4.02	4.02	4.13	3.93	4.05	3.86	3.93	3.96	4.15	3.85	3.93
6.02	7.04	6.75	8.11	8.00	7.14	6.67	7.08	8.18	7.25	12.67	8.22	7.38	7.44	7.71	7.85
2.27	2.73	2.39	2.76	2.24	2.07	2.96	2.86	2.36	2.35	2.44	2.22	2.17	3.35	2.14	2.81
3.31	3.26	3.36	3.16	3.11	3.26	3.37	3.20	3.03	3.21	2.75	3.01	3.30	3.06	3.05	2.93
0.15	0.15	0.14	0.15	0.15	0.14	0.15	0.15	0.15	0.15	0.15	0.15	0.14	0.15	0.15	0.15
12.33	12.65	14.39	15.63	14.98	14.79	13.53	15.06	14.59	14.62	19.98	14.66	14.07	16.09	13.82	14.60

Please cite this article as: Perri, F., et al., Provenance and accommodation pathways of late Quaternary sediments in the deep-water northern Ionian Basin, southern Italy, Sediment. Geol. (2012), doi:10.1016/j.sedgeo.2012.01.007

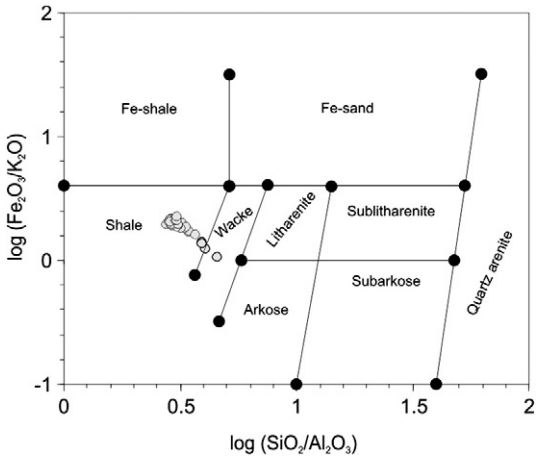

Fig. 5. Classification diagram for the studied mud samples (Herron, 1988).

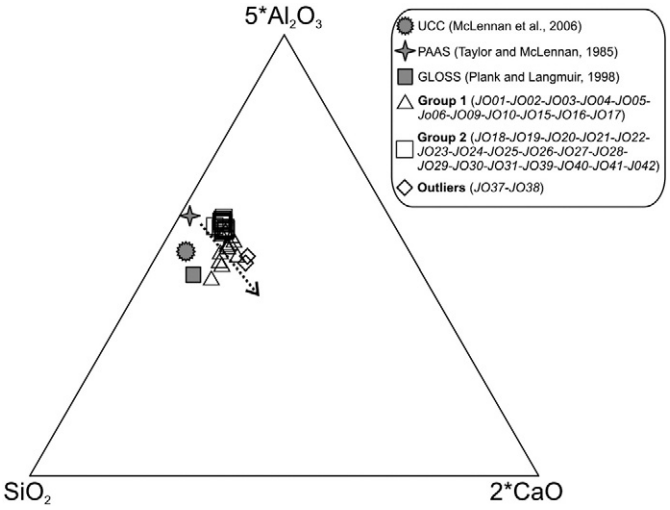

Fig. 7. Ternary plot showing the relative proportions of SiO_2 (representing quartz or opaline silica), Al_2O_3 (representing mica/clay minerals), and CaO (representing carbonate) for the studied mud samples.

sand of the Lipuda and Nicà Rivers, or from carbonate sand of local intrabasinal highs and eroded late Quaternary terraces, at the southern end of the studied area.

The Ionian Calabria margin is a typical tectonically active siliciclastic continental margin, with canyon-fed sources supplemented by smaller-scale failures coming off steep slopes adjacent to the coastline. Identification of source areas and flow pathways has revealed single sources for sand and mud turbidites; nonetheless, northeastward-flowing bottom currents may have some influence on the widespread distribution of muddy deposits.

In summary, studies of modern sedimentary systems illustrate the complexity of variables controlling sand composition, especially in transform settings with diverse source rocks, relief, transport mechanisms and depositional settings. Evaluation of these effects, dispersal pathways and detrital modes using a transect extending from mountainous sources to deep-marine depositional sites improves our understanding of sediment production, transport and ultimate composition. First- and second-order sands (e.g., Ingersoll et al., 1993) directly reflect local source rocks and are most useful in local paleogeographic and paleotectonic reconstructions, and to infer distinctive climatic/paleoclimatic signatures. In contrast, third-order sand from the ultimate site of deposition represents the sum of all processes acting in mountain ranges, streams, rivers and the marine environment, and are, thus, more useful in determining overall tectonic setting.

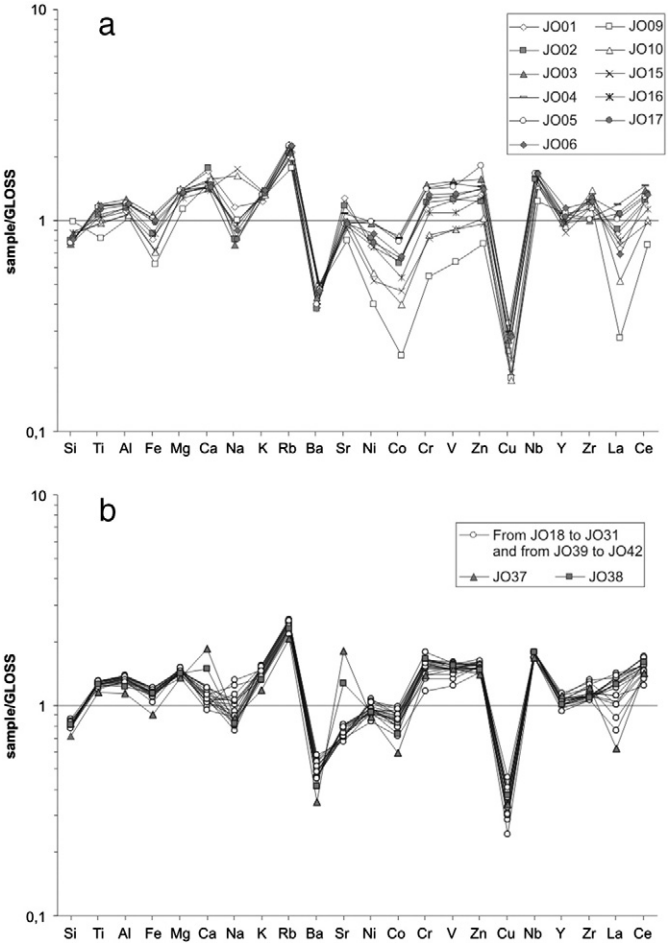

Fig. 6. Distribution of the major and trace elements for the studied mud samples normalized to the Global Subducting Sediment (GLOSS; Plank and Langmuir, 1998).

Acknowledgments

This research has been carried out within the MIUR-ex60% Projects (Palaeogeographic and Palaeotectonic Evolution of the Circum-Mediterranean Orogenic Belts, 2001–2005; and Relationships between Tectonic Accretion, Volcanism and Clastic Sedimentation within the Circum-Mediterranean Orogenic Belts, 2006–2011; Resp. S. Critelli), the 2006–2008 MIUR-PRIN Project 2006.04.8397 'The Cenozoic clastic

Table 5
The LREEs/M ratios, where M is a transition element (Cr and Ni), for the studied mud samples compared to the most important basement rocks drained by the Calabrian rivers.

Elemental ratios	Range of studied mud sediments		Range of Calabrian basement rocks[a]		Upper continental crust[b]	Post-Archean Australian average shale[c]
	Area 1	Area 2	Felsic rocks	Mafic rocks		
(La + Ce)/Cr	0.93–1.34	0.83–1.16	0.88–4.11	0.01–0.15	1.13	1.07
(La + Ce)/Ni	1.50–2.21	1.57–1.98	2.16–5.65	0.01–0.31	2.13	2.14
Ni/(La + Ce)	0.74–1.08	0.87–1.20	0.26–1.23	1.95–6.69	0.47	0.46

[a] Ayuso et al., 1994; Fornelli et al., 2007; Perri et al., 2011b.
[b] McLennan et al., 2006.
[c] Taylor and McLennan, 1985.

sedimentation within the Circum-Mediterranean orogenic belts: implications for palaeogeographic and palaeotectonic evolution' (Resp. S. Critelli), and the OGS funded projects WGDT (Morphology and Architecture of the Western Portions of the Gulf of Taranto: a Study of Submarine Instability in a Tectonically Active Margin; Resp. S. Critelli). The authors are indebted to Robert Cullers and Abhijit Basu and the Guest Editor Raymond V. Ingersoll for their reviews and suggestions.

References

Ayuso, R.A., Messina, A., De Vivo, B., Russo, S., Woodruff, L.G., Sutter, J.F., Belkin, H.E., 1994. Geochemistry and argon thermochronology of the Variscan Sila Batholith, southern Italy: source rocks and magma evolution. Contributions to Mineralogy and Petrology 117, 87–109.

Barone, M., Critelli, S., Dominici, R., Muto, F., 2008. Detrital modes in a late Miocene wedge-top basin, northeastern Calabria, Italy: compositional record of wedge-top partitioning. Journal of Sedimentary Research 78, 693–711.

Basu, A., 1976. Petrology of Holocene fluvial sand derived from plutonic source rocks: implications to paleoclimatic interpretation. Journal of Sedimentary Petrology 46, 694–709.

Basu, A., 1985. Reading provenance from detrital quartz. In: Zuffa, G.G. (Ed.), Provenance of Arenites. D. Reidel Publishing, Boston, pp. 231–247.

Bauluz, B., Mayayo, M.J., Fernandez-Nieto, C., Gonzalez Lopez, J.M., 2000. Geochemistry of Precambrian and Paleozoic siliciclastic rocks from the Iberian Range (NE Spain): implications for source-area weathering, sorting, provenance, and tectonic setting. Chemical Geology 168, 135–150.

Bernasconi, M.P.E., Le Pera, E., Critelli, S., Randazzo, G., Amore, C., 2002. Caratteri sedimentologici ed ecologici del Delta del Fiume Neto, Calabria Orientale. Studi Geologici Camerti 17, 1–13.

Boccaletti, M., Nicolich, R., Tortrici, L., 1984. The Calabrian Arc and the Ionian sea in the dynamic evolution of the central Mediterranean. Marine Geology 55, 219–245.

Caracciolo, L., Le Pera, E., Muto, F., Perri, F., 2011. Sandstone petrology and mudstone geochemistry of the Peruc–Korycany Formation (Bohemian Cretaceous Basin, Czech Republic). International Geology Review 53, 1003–1031.

Cavalcante, F., Fiore, S., Lettino, A., Piccarret, G., Tateo, F., 2007. Illite–smective mixed layers in sicilide shales and piggy-back deposits of the Gorgoglione Formation (Southern Apennines): geological inferences geodynamic implications. Bollettino della Societa Geologica Italiana 126, 241–254.

Cavazza, W., Ingersoll, R.V., 2005. Detrital modes of the Ionian forearc basin fill (Oligocene–Quaternary) reflect the tectonic evolution of the Calabria–Peloritani terrane (southern Italy). Journal of Sedimentary Research 75, 268–379.

Condie, K.C., Noll, P.D.J., Conway, C.M., 1992. Geochemical and detrital mode evidence for two sources of early Proterozoic sedimentary rocks from the Tonto Basin Supergroup, central Arizona. Sedimentary Geology 77, 51–76.

Condie, K.C., Lee, D., Farmer, G.L., 2001. Tectonic setting and provenance of the Neoproterozoic Uinta Mountain and Big Cottonwood groups, northern Utah: constraints from geochemistry, Nd isotopes, and detrital modes. Sedimentary Geology 141, 443–464.

Critelli, S., 1999. The interplay of lithospheric flexure and thrust accommodation in forming stratigraphic sequences in the southern Apennines foreland basin system, Italy. Memorie dell'Accademia Nazionale dei Lincei 10, 257–326.

Critelli, S., Le Pera, E., 1998. Post-Oligocene sediment dispersal systems and unroofing history of the Calabrian microplate, Italy. International Geology Review 40, 609–637.

Critelli, S., Le Pera, E., 2003. Provenance relations and modern sand petrofacies in an uplifted thrust-belt, northern Calabria, Italy. In: Valloni, R., Basu, A. (Eds.), Quantitative Provenance Studies in Italy: Servizio Geologico Nazionale, Memorie Descrittive della Carta Geologica d'Italia, 61, pp. 25–38.

Critelli, S., Mongelli, G., Perri, F., Martin-Algarra, A., Martin-Martin, M., Perrone, V., Dominici, R., Sonnino, M., Zaghloul, M.N., 2008. Compositional and geochemical signatures for the sedimentary evolution of the Middle Triassic–Lower Jurassic continental redbeds from western-central Mediterranean Alpine chains. Journal of Geology 116, 375–386.

Critelli, S., Muto, F., Tripodi, V., Perri, F., 2011. Relationships between lithospheric flexure, thrust tectonics and stratigraphic sequences in foreland setting: the southern Apennines foreland basin system, Italy. In: Schattner, U. (Ed.), New Frontiers in Tectonic Research — At the Midst of Plate Convergence. InTech Open Access Publisher, pp. 121–170.

Cullers, R.L., Barrett, T., Carlson, R., Robinson, B., 1987. Rare-earth element and mineralogic changes in Holocene soil and stream sediment: a case study in the West Mountains, Colorado, U.S.A. Chemical Geology 70, 335–348.

Cullers, R.L., Basu, A., Suttner, L.J., 1988. Geochemical signature of provenance in sand-size material in soils and stream sediments near the Tobacco Root batholith, Montana, U.S.A. Chemical Geology 70, 335–348.

Dickinson, W.R., 1970. Interpreting detrital modes of greywacke and arkose. Journal of Sedimentary Petrology 40, 695–707.

Elderfield, H., 1976. Hydrogenous material in marine sediments: excluding manganese nodules. In: Riley, J.P., Chester, R. (Eds.), Chemical Oceanography, 5. Academic Press, London, pp. 137–215.

Fornelli, A., Micheletti, F., Piccarreta, G., 2007. The Neoproterozoic–Early Cambrian felsic magmatism in Calabria (Italy): inferences as to the origin and geodynamic setting. Periodico di Mineralogia 76, 99–112.

Franzinelli, E., Potter, P.E., 1983. Petrology, chemistry and texture of modern river sand, Amazon River system. Journal of Geology 91, 23–39.

Franzini, M., Leoni, L., Saitta, M., 1972. A simple method to evaluate the matrix effects in X-ray fluorescence analysis. X-Ray Spectrometry 1, 151–154.

Franzini, M., Leoni, L., Saitta, M., 1975. Revisione di una metodologia analitica per fluorescenza-X, basata sulla correzione completa degli effetti di matrice. Rendiconti della Società Italiana di Mineralogia e Petrologia 31, 365–378.

Gazzi, P., 1966. Le arenarie del Flysch sopracretaceo dell'Appennino modenese; correlazioni con il Flysch di Monghidoro. Mineralogica et Petrografica Acta 12, 69–97.

Grantham, J.H., Velbel, M.A., 1988. The influence of climate and topography on rock-fragment abundance in modern fluvial sands of the southern Blue Ridge Mountains, North Carolina. Journal of Sedimentary Petrology 58, 219–227.

Guerricchio, A., Melidoro, G., 1975. Geological investigations applied to the archaeology of the buried city of Sybaris. Bulletin of International Association of Engineering Geology 12, 83–88.

Herron, M.M., 1988. Geochemical classification of terrigenous sands and shales from core or log data. Journal of Sedimentary Petrology 58, 820–829.

Ingersoll, R.V., Bullard, T.F., Ford, R.L., Grimm, J.P., Pickle, J.D., Sares, S.W., 1984. The effect of grain size on detrital modes: a test of the Gazzi–Dickinson point-counting method. Journal of Sedimentary Petrology 54, 103–116.

Ingersoll, R.V., Kretchmer, A.G., Valles, P.K., 1993. The effect of sampling scale on actualistic sandstone petrofacies. Sedimentology 40, 937–953.

Johnsson, M.J., 1990. Overlooked sedimentary particles from tropical weathering environments. Geology 18, 107–110.

Johnsson, M.J., 1993. The system controlling the composition of clastic sediments. In: Johnsson, M.J., Basu, A. (Eds.), Processes controlling the composition of clastic sediments: Geological Society of America, Special Paper, 284, pp. 1–19.

Johnsson, M.J., Stallard, R.F., 1989. Physiographic controls on the composition of sediments derived from volcanic and sedimentary terrains on Barro Colorado Island, Panama. Journal of Sedimentary Petrology 59, 768–781.

Johnsson, M.J., Stallard, R.F., Meade, R.H., 1988. First-cycle quartz arenites in the Orinoco River basin, Venezuela and Colombia. Journal of Geology 96, 263–277.

Karbassi, A.R., Amirnezhad, R., 2004. Geochemistry of heavy metals and sedimentation rate in a bay adjacent to the Caspian Sea. International journal of Environmental Science and Technology 1, 199–206.

Knott, S.D., Turco, E., 1991. Late Cenozoic kinematics of the Calabrian Arc, southern Italy. Tectonics 10, 1164–1172.

Krumm, S., 1996. WINFIT 1.2: version of November 1996 (The Erlangen geological and mineralogical software collection) of "WINFIT 1.0: a public domain program for interactive profile-analysis under WINDOWS". XIII Conference on Clay Mineralogy and Petrology, Praha, 1994: Acta Univers itatis Carolinae Geologica, 38, pp. 253–261.

Le Pera, E., Sorriso Valvo, M., 2000. Weathering and morphogenesis in a Mediterranean climate, Calabria, Italy. Geomorphology 34, 251–270.

Le Pera, E., Arribas, J., Critelli, S., Tortosa, A., 2001. The effects of source rocks and chemical weathering on the petrogenesis of siliciclastic sand from the Neto River (Calabria, Italy): implications for provenance studies. Sedimentology 48, 357–377.

Leoni, L., Saitta, M., 1976a. Determination of yttrium and niobium on standard silicate rocks by X-ray fluorescence analyses. X-Ray Spectrometry 5, 29–30.

Leoni, L., Saitta, M., 1976b. X-ray fluorescence analysis of 29 trace elements in rock and mineral standards. Rendiconti della Società Italiana di Mineralogia e Petrologia 32, 497–510.

Mann, W.R., Cavaroc, V.V., 1973. Composition of sand released from three source areas under humid, low-relief weathering in the North Carolina piedmont. Journal of Sedimentary Petrology 43, 870–881.

McLennan, S.M., Taylor, S.R., 1991. Sedimentary rocks and crustal evolution: tectonic setting and secular trends. Journal of Geology 99, 1–21.

McLennan, S.M., Taylor, S.R., Hemming, S.R., 2006. Composition, differentiation, and evolution of continental crust: constrains from sedimentary rocks and heat flow. In: Brown, M., Rushmer, T. (Eds.), Evolution and Differentiation of the Continental Crust. Cambridge University Press, pp. 92–134.

Mongelli, G., Critelli, S., Perri, F., Sonnino, M., Perrone, V., 2006. Sedimentary recycling, provenance and paleoweathering from chemistry and mineralogy of Mesozoic continental redbed mudrocks, Peloritani Mountains, Southern Italy. Geochemical Journal 40, 197–209.

Moore, D.M., Reynolds, R.C., 1997. X-ray Diffraction and Identification and Analysis of Clay Minerals. Oxford University Press, Oxford.

Nesbitt, H.W., Young, G.M., 1982. Early Proterozoic climates and plate motions inferred from major element chemistry of lutites. Nature 299, 715–717.

Nesbitt, H.W., Young, G.M., McLennan, S.M., Keays, R.R., 1996. Effects of chemical weathering and sorting on the petrogenesis of siliciclastic sediments, with implications for provenance studies. Journal of Geology 104, 525–542.

Nichols, G., 1999. Sedimentology and Stratigraphy. Blackwell Science Ltd, London, p. 355.

Perri, F., Mongelli, G., Sonnino, M., Critelli, S., Perrone, V., 2005. Chemistry and mineralogy of Mesozoic continental redbed mudrocks from the Calabrian Arc, Southern Italy: implication for provenance, paleoweathering and burial history. Atti Ticinensi di Scienze della Terra 10, 103–106.

Perri, F., Cirrincione, R., Critelli, S., Mazzoleni, P., Pappalardo, A., 2008. Clay mineral assemblages and sandstone compositions of the Mesozoic Longobucco Group (north-eastern Calabria): implication for burial history and diagenetic evolution. International Geology Review 50, 1116–1131.

Perri, F., Critelli, S., Mongelli, G., Cullers, R.L., 2011a. Sedimentary evolution of the Mesozoic continental redbeds using geochemical and mineralogical tools: the case of Upper Triassic to Lowermost Jurassic M.te di Gioiosa mudstones (Sicily, Southern Italy). International Journal of Earth Sciences 100, 1569–1587.

Perri, F., Muto, F., Belviso, C., 2011b. Links between composition and provenance of Mesozoic siliciclastic sediments from Western Calabria (Southern Italy). Italian Journal of Geosciences 130, 318–329.

Please cite this article as: Perri, F., et al., Provenance and accommodation pathways of late Quaternary sediments in the deep-water northern Ionian Basin, southern Italy, Sediment. Geol. (2012), doi:10.1016/j.sedgeo.2012.01.007

Plank, T., Langmuir, C.H., 1998. The chemical composition of subducting sediment and its consequences for the crust and mantle. Chemical Geology 145, 325–394.
Potter, P.E., 1978. Petrology and chemistry of big river sands. Journal of Geology 86, 423–449.
Romagnoli, C., Gabbianelli, G., 1990. Late Quaternary sedimentation and soft-sediment deformations in the Corigliano Basin (Gulf of Taranto, northern Ionian Sea). Giornale di Geologia 52, 33–53.
Rossi, S., Sartori, R., 1981. A seismic reflection study of the External Calabrian Arc in the Northern Ionian Sea (Eastern Mediterranean). Marine Geophysical Researches 4, 403–426.
Sartori, R., 2003. The Tyrrhenian back arc basin and subduction of the Ionian lithosphere. Episodes 2683, 217–221.
Stallard, R.F., 1988. Weathering and erosion in the humid tropics. In: Lerman, A., Meybeck, M. (Eds.), Physical and Chemical Weathering in Geochemical Cycles. : NATO ASI Series C: Mathematical and Physical Sciences, 251. Kluwer Academic Publishers, Dordrecht, Holland, pp. 225–246.
Suttner, L.J., 1974. Sedimentary petrographic province: an evaluation. Society of Economic Paleontologists and Mineralogists Special Publication 21, 75–84.
Suttner, L.J., Basu, A., Mack, G.H., 1981. Climate and the origin of quartz arenites. Journal of Sedimentary Petrology 51, 1235–1246.
Tansi, C., Muto, F., Critelli, S., iovine, G., 2007. Neogene–Quaternary strike–slip tectonics in the central Calabria Arc (southern Italy). Journal of Geodynamics 43, 397–414.
Taylor, S.R., McLennan, S.M., 1985. The Continental Crust: Its Composition and Evolution. Blackwell Sciences Publication.
Van Dijk, J.P., Bello, M., Brancaleoni, G.P., Cantarella, G., Costa, V., Frixa, A., Golfetto, F., Merlini, S., Riva, M., Torricelli, S., Toscano, C., Zerilli, A., 2000. A regional structural model for the northern sector of the Calabria Arc (Southern Italy). Tectonophysics 324, 267–320.
Velbel, M.A., 1985. Hydrogeochemical constrains on mass balances in forested watersheds on the southern Appalachians. In: Drever, J.L. (Ed.), The Chemistry of Weathering. D. Reidel, Holland, pp. 231–247.
Zaghloul, M.N., Critelli, S., Perri, F., Mongelli, G., Perrone, V., Sonnino, M., Tucker, M., Aiello, M., Ventimiglia, C., 2010. Depositional systems, composition and geochemistry of Triassic rifted continental margin redbeds of Internal Rif Chain, Morocco. Sedimentology 57, 312–350.
Zecchin, M., Civile, D., Caffau, M., Roda, C., 2009. Facies and cycle architecture of a Pleistocene marine terrace (Crotone, southern Italy): a sedimentary response to late Quaternary, high-frequency glacio-eustatic changes. Sedimentary Geology 216, 138–157.
Zecchin, M., Ceramicola, S., Gordini, E., Deponte, M., Critelli, S., 2011. Cliff overstep model and variability in the geometry of transgressive erosional surfaces in high-gradient shelves: the case of the Ionian Calabrian margin (southern Italy). Marine Geology 281, 43–58.
Zuffa, G.G., 1985. Optical analyses of arenites: influence of methodology on compositional results. In: Zuffa, G.G. (Ed.), Provenance of Arenites. Dordrecht, The Netherlands, NATO Advanced Study Institute Series, Reidel, 148, pp. 165–189.

Please cite this article as: Perri, F., et al., Provenance and accommodation pathways of late Quaternary sediments in the deep-water northern Ionian Basin, southern Italy, Sediment. Geol. (2012), doi:10.1016/j.sedgeo.2012.01.007